

Article

Empirical Modeling of Viscosities and Softening Points of Straight-Run Vacuum Residues from Different Origins and of Hydrocracked Unconverted Vacuum Residues Obtained in Different Conversions

Dicho Stratiev ^{1,*}, Svetoslav Nenov ², Dimitar Nedanovski ³, Ivelina Shishkova ¹, Rosen Dinkov ¹, Danail D. Stratiev ⁴, Denis D. Stratiev ⁵, Sotir Sotirov ⁵, Evdokia Sotirova ⁵, Vassia Atanassova ⁴, Simeon Ribagin ^{4,5}, Krassimir Atanassov ^{4,5}, Dobromir Yordanov ⁵, Nora A. Angelova ³ and Liliana Todorova-Yankova ⁵

- ¹ LUKOIL Neftohim Burgas, 8104 Burgas, Bulgaria; shishkova.ivelina.k@neftochim.bg (I.S.); dinkov.rosen.k@neftochim.bg (R.D.)
 - ² Department of Mathematics, University of Chemical Technology and Metallurgy, Kliment Ohridski 8, 1756 Sofia, Bulgaria; s.nenov@gmail.com
 - ³ Faculty of Mathematics and Informatics, University "St. Kliment Ohridski", 15 Tsar Osvoboditel Blvd., 1504 Sofia, Bulgaria; dnedanovski@fmi.uni-sofia.bg (D.N.); nora.angelova@fmi.uni-sofia.bg (N.A.A.)
 - ⁴ Institute of Biophysics and Biomedical Engineering, Bulgarian Academy of Sciences, Academic Georgi Bonchev 105, 1113 Sofia, Bulgaria; danail.stratiev@gmail.com (D.D.S.); vassia.atanassova@gmail.com (V.A.); sim_ribagin@mail.bg (S.R.); k.t.atanassov@gmail.com (K.A.)
 - ⁵ Intelligent Systems Laboratory, Department Industrial Technologies and Management, University of Chemical Technology and Metallurgy, Kliment Ohridski 8, 1756 Sofia, Bulgaria; aitos_dsdd@abv.bg (D.D.S.); ssotirov@btu.bg (S.S.); esotirova@btu.bg (E.S.); dobromirj@abv.bg (D.Y.); litoian@abv.bg (L.T.-Y.)
- * Correspondence: stratiev.dicho@neftochim.bg



Citation: Stratiev, D.; Nenov, S.; Nedanovski, D.; Shishkova, I.; Dinkov, R.; Stratiev, D.D.; Stratiev, D.D.; Sotirov, S.; Sotirova, E.; Atanassova, V.; et al. Empirical Modeling of Viscosities and Softening Points of Straight-Run Vacuum Residues from Different Origins and of Hydrocracked Unconverted Vacuum Residues Obtained in Different Conversions. *Energies* **2022**, *15*, 1755. <https://doi.org/10.3390/en15051755>

Academic Editors: Ricardo J. Bessa and Edo Boek

Received: 9 December 2021

Accepted: 22 February 2022

Published: 26 February 2022

Publisher's Note: MDPI stays neutral with regard to jurisdictional claims in published maps and institutional affiliations.



Copyright: © 2022 by the authors. Licensee MDPI, Basel, Switzerland. This article is an open access article distributed under the terms and conditions of the Creative Commons Attribution (CC BY) license (<https://creativecommons.org/licenses/by/4.0/>).

Abstract: The use of hydrocracked and straight-run vacuum residues in the production of road pavement bitumen requires a good understanding of how the viscosity and softening point can be modeled and controlled. Scientific reports on modeling of these rheological properties for hydrocracked and straight-run vacuum residues are scarce. For that reason, 30 straight-run vacuum residues and 33 hydrocracked vacuum residues obtained in a conversion range of 55–93% were investigated, and the characterization data were employed for modeling purposes. An intercriteria analysis was applied to investigate the statistically meaningful relations between the studied vacuum residue properties. It revealed that the straight-run and hydrocracked vacuum residues were completely different, and therefore their viscosity and softening point should be separately modeled. Through the use of nonlinear regression by applying CAS Maple and NLPsolve with the modified Newton iterative method and the vacuum residue bulk properties the viscosity and softening point were modeled. It was found that the straight-run vacuum residue viscosity was best modeled from the molecular weight and specific gravity, whereas the softening point was found to be best modeled from the molecular weight and C₇-asphaltene content. The hydrocracked vacuum residue viscosity and softening point were modeled from a single property: the Conradson carbon content. The vacuum residue viscosity models developed in this work were found to allow prediction of the asphaltene content from the molecular weight and specific gravity with an average absolute relative error of 20.9%, which was lower of that of the model of Samie and Mortaheb (*Fuel*. 2021, 305, 121609)—32.6%.

Keywords: vacuum residue; hydrocracked vacuum residue; intercriteria analysis; empirical modeling; asphaltenes; viscosity; softening point

1. Introduction

The vacuum residue (VR) is the part of petroleum that is the most difficult to process and analyze. The inclination of some compounds to aggregate and precipitate is the most

challenging process characteristic of vacuum residues. The aggregation and sedimentation are associated with a shorter process unit cycle length and unplanned shutdowns with huge loss of profit opportunity for oil refining [1–3]. The lower fluidity and volatility make vacuum residues difficult to analyze. For that reason, sometimes strange values for a VR's physicochemical properties are reported [4,5]. The proper preparation of a VR sample before analyzing is important to reduce the probability of misinterpretation of the obtained results [5,6]. For example, the most complex compounds of a VR—the asphaltenes—were believed to consist predominantly of molecules with one polycyclic aromatic hydrocarbon (PAH) unit per molecule, with roughly 7 rings having a structure “like your hand” (palm), which has a small number of aliphatic chains (fingers) [7]. The “like your hand” model is also called the “island” or “continental” model [7]. Matching the ubiquitous asphaltene spectral data with molecular orbital calculations showed that asphaltene ring systems predominantly consist of 4–10 rings. PAHs with 6–8 rings are the most predominant in petroleum asphaltenes [7,8]. The research group of Mullins, based on time-resolved fluorescence depolarization (TRFD) studies, refuted the “archipelago” for the bulk of asphaltene [7]. They concluded that asphaltenes are polydisperse, and as such there will be some fraction of asphaltene molecules containing two fused rings, and a much smaller asphaltene fraction containing three fused rings [8]. Chacón-Patiño et al. [9–11], however, revealed that by a preliminary fractionation of the asphaltene sample before analyzing it by positive-ion atmospheric pressure photoionization, Fourier-transform ion cyclotron resonance mass spectrometry, and infrared multiphoton dissociation, the island and archipelago motifs coexist in petroleum asphaltenes. Moreover, they demonstrated that mass spectrometry analysis of asphaltenic samples is biased toward the preferential ionization/detection of island structural motifs, and that this bias explains the overwhelming mass spectral support of the island model. They showed that the asphaltene structure is a continuum of island and archipelago motifs, and hypothesized that the dominant structure (island or archipelago) depends upon the asphaltene sample. These findings based on spectral techniques, which were registered after a preliminary step of asphaltene fractionation, disproved the belief adopted by many researchers also using spectral techniques [12–16] that the asphaltene structure is “like your hand” (island model). The molecular weight of the VR and its constituents is important information when researching the optimal conditions to process a particular VR. Despite the criticized vapor pressure osmometry (VPO) method to measure asphaltene's molecular weight, Wiehe showed that when a strong polar solvent is used and the temperature of measurement is sufficiently high, no dependence of the asphaltene's molecular weight on the asphaltene concentration was observed [17]. This can be considered as an indicator that the molecular weight measured by VPO and high polarity solvent at temperature of 130 °C asphaltene should be that of the asphaltene monomer molecular weight [17]. Regardless of the internecine scientific wars [7,18] over the molecular weight of the asphaltenes, one thing is clear: as a whole, the VR constituents (SARA fractions) have diverse molecular weights depending on the petroleum's origin. This is well exemplified by the data in Table 1, which was extracted from the literature sources [19–23].

Table 1. Variation in molecular weights of VR and its SARA fractions reported in [19–23].

Vacuum Residue and Its SARA Fractions	Minimal Molecular Weight, g/mol	Maximal Molecular Weight, g/mol
Whole vacuum residue	581 Russia (Akbarzadeh et al., 2005 [19])	2500 Arab. Heavy (Schucker, 1983 [20])
Saturates	361 Russia (Akbarzadeh et al., 2005 [19])	900 Arab. Heavy (Schucker, 1983 [20])
Aromatics	450 Russia (Akbarzadeh et al., 2005 [19])	1080 Daqing (Liang et al., 2000 [21])

Table 1. Cont.

Vacuum Residue and Its SARA Fractions	Minimal Molecular Weight, g/mol	Maximal Molecular Weight, g/mol
Resins	775 Columbian VR2 (León et al., 2008 [22])	1900 Arab. Heavy (Schucker, 1983 [19])
Asphaltenes	750 [7]	4190 ± 630 Athabasca (Sheremata et al. [23])

The molecular weight of petroleum and its fractions was shown in several developed correlations that depended on average boiling point, or T_{50%}, and specific gravity (SG), or density [24–27]. Therefore, the T_{50%} of the VR, along with the VR's SG, can be used to estimate the VR molecular weight. Moreover, the T_{50%} and SG were shown in our recent studies [28,29] to be the most informative properties of heavy oils that correlated with aromatic carbon and hydrogen contents, saturate contents, polynuclear aromatic content, and viscosity of vacuum gas oils. Therefore, one may expect that the same VR characteristics can be used to correlate with the other important VR physicochemical properties that give information about the chemical nature of the vacuum residue. Unfortunately, the determination of the VR's T_{50%} can be problematic when high-temperature simulated distillation (HTSD) is used, due to the inability of the entire amount of the VR sample to evaporate and enter the gas chromatographic column [30,31]. In this work, we employed HTSD to measure the distillation characteristics of diverse vacuum residues, and the continuous boiling point distribution model of Riazi [32] was applied to atmospheric residue distillation data to estimate the VR's T_{50%}. Then, we used this information to calculate the VR's molecular weight and to model the VR's rheological properties: viscosity and softening point. We also employed intercriteria analysis (ICrA) to evaluate the presence of statistically meaningful relations between the different physicochemical properties of 30 straight-run VRs originating from extra light to extra heavy petroleum from all over the world. Additionally, the relations between the different physicochemical properties of 33 hydrocracked unconverted vacuum residues (H-Oil VTBs) obtained at conversions between 58% and 93% were examined by ICrA, and the extent of similarities between the H-Oil VTBs and the SRVRs were defined by ICrA.

Irvin Wiehe's thought deserves mentioning here: "Petroleum is so complex with a high degree of uncertainty that no concept is definite." [33]. An example of the uncertainty of VR asphaltene molecular weight measurement was discussed above. Another example of an incorrect report on the measured density of VR can be found in our earlier research [5]. In order to avoid the incorrect measurement of the VR densities, the investigated VRs were diluted with toluene at concentrations from 0.01 to 0.06 kg/L. The density of the VRs were calculated using a mixing rule as explained in [34,35]. The accuracy of the VR viscosity measurement is another uncertainty. The accuracy and repeatability of VR viscosity measurements are affected by the selection of viscometers and the experimental procedures followed by different operators [4,36]. A study published by Miller et al. [4] indicated that heavy oil viscosities measured by different viscometers, or by the same type of viscometer but measured in different laboratories following different operating procedures, were found to be quite different. The inconsistency of the measured viscosities makes data interpretation very difficult. Moreover, Samie and Mortaheb [37] developed correlations to predict VR SARA composition from the VR properties: density, Conradson carbon content, and viscosity, and an incorrect viscosity measurement will lead to an incorrect SARA analysis prediction. In order to avoid inconsistency in the measured viscosities of the distinct studied VRs, a dilution with 30% fluid catalytic cracking (FCC) heavy cycle oil (HCO) was applied. This method, as shown in the research of Samie and Mortaheb [37], can provide a reliable basis for VR property modeling.

Petroleum refining seeks a suitable application of secondary unconverted vacuum residues. Such an application can be the use of the secondary unconverted vacuum residues

as feed components for road asphalt production [38,39]. Due to a lack of knowledge of their rheological property variations with conversion level alterations and the degree of similarity or dissimilarity with the rheological properties of the straight-run vacuum residues from different origins, the involvement of the secondary vacuum residues in the process of road asphalt production is still limited. The modeling of the rheological properties of the primary and the secondary vacuum residues can help increase the share of low-value secondary residues in the road pavement bitumen by proper blending of hydrocracked vacuum residues with the suitable straight-run vacuum residues in the optimum ratio from an economical and technological point of view.

To the best of our knowledge, no reports have appeared in the literature that modeled the viscosity and softening point of primary and secondary (hydrocracked) vacuum residues, the properties of which vary in a wide range. To fill this gap, an attempt was made in this study to define the characteristics of the *SRVRs* and the hydrocracked vacuum residues that have statistically meaningful relations as evaluated by the use of intercriteria analysis, which can be used for viscosity and softening-point modeling. An evaluation of the extent of similarities between the primary and secondary vacuum residual oils based on the application of an intercriteria analysis was also performed in this research to define the most appropriate approach to modeling the viscosity and softening point. Among the defined statistically meaningful relations between the vacuum residue bulk properties with viscosity and softening point employed to model the rheological properties, the VR bulk characteristics that most accurately predicted both viscosity and softening point were distinguished. The aim of the current study was to discuss the obtained results and define the most suitable models to predict the viscosity and softening point that can be used in the process of optimization of feed composition that contains straight-run and hydrocracked vacuum residual oils for production of road asphalt

2. Materials and Methods

The studied 30 straight-run vacuum residues (*SRVRs*) were obtained by TBP distillation of crude oils and atmospheric residual oils (*AROs*) in the research laboratory of LUKOIL Neftohim Burgas (LNB). The atmospheric part of the TBP distillation was performed in accordance with ASTM D 2892, while the vacuum part of the TBP distillation was carried out in accordance with ASTM D 5236. The *SRVRs* were the fractions of the crudes that boiled above 540 °C. The hydrocracked vacuum residual oils, also named H-Oil vacuum tower bottoms (*VTBs*), were obtained from the LNB H-Oil vacuum residue hydrocracking during processing of the *SRVRs*. The methods used to measure the vacuum residues' properties are explained in our recent work [40]. Densities of the vacuum residual oils were measured indirectly from the densities of a series of solutions of asphaltenes and vacuum residues in toluene at different concentrations, as described in [40]. Solutions of vacuum residues in toluene at concentrations up to a vacuum residue mass fraction of 6% were prepared. Properties of crudes and the *SRVRs* obtained therefrom are presented in Table 2. Table 3 summarizes the properties of the 33 H-Oil *VTB* products under study. The data for the vacuum residue densities reported in Tables 2 and 3 were obtained by dilution with toluene. The repeatability of the density measurement by dilution with toluene was 0.0035 g/cm³ for the vacuum residual oils.

Table 2. Physicochemical properties of *SRVRs* and of the crude oils from which they originated.

Crude Origin	Crude d 15 °C, g/cm ³	Crude Sulfur, %	>540 °C, wt. %	VR SG	VR Concarbon, wt. %	VR Sulfur, %	Sat, wt. %	Aro, wt. %	Res, wt. %	C ₇ -Asp, wt. %	C ₅ -Asp, wt. %	Kin. Vis., mm ² /s *	Soft Point, °C	IBP	10%	30%	50%	70%	90%	95%	FBP	MW	ARI
Urals	0.877	1.53	25.2	0.997	17.5	3.0	25.6	52.5	7.8	14.1	17.6	220.9	40.1	540	559	602	657	735	884	961	1130	808	4.0
Arab Med.	0.872	2.48	25.2	1.031	20.7	5.4	11.8	68.3	5.3	14.6	25.5	338.3	44.7	538	560	608	670	758	927	1016	1217	840	5.2
Arab Heavy	0.889	2.91	32.0	1.040	23.6	5.8	12.4	61.9	4.4	21.3	32.9	374.6	51.2	538	565	628	709	827	1060	1186	1486	953	5.9
Val'Dagri	0.832	1.97	14.6	1.052	21.4	6.0	11.7	73.5	6.4	8.5	19.5	219.3	43.7	538	554	593	643	715	857	931	1086	764	5.5
Basrah L	0.878	2.85	28.3	1.052	23.8	5.9	12.3	64.8	4.9	18.0	27.7	368.9	50.3	539	562	616	684	782	969	1069	1297	877	6.0
Basrah H	0.905	3.86	33.8	1.071	28.9	7.1	12.3	54.1	5.8	27.7	37.0	731.9	68.6	539	567	632	715	836	1072	1200	1504	968	6.9
Kirkuk	0.873	2.65	24.6	1.054	25.2	5.9	15.2	55.4	5.0	24.3	33.1	514.1	58.1	539	561	611	676	769	950	1046	1264	853	5.9
Iranian H	0.882	2.27	28.1	1.050	23.9	5.2	17.0	52.6	5.0	25.4	36.2	528.6	61.9	540	561	609	668	751	908	989	1171	832	5.7
KEB	0.876	2.64	27.7	1.037	23.3	5.7	15.0	64.2	4.2	16.6	25.7	392.3	47.8	540	561	608	667	749	901	980	1157	830	5.3
El Bouri	0.891	1.76	26.2	1.050	25.5	3.3	12.0	57.9	12.6	17.5	27.3	303.0	45.0	538	558	605	666	756	931	1024	1231	827	5.7
Kazakh H	0.858	0.81	23.7	0.990	17.1	1.7	33.0	50.2	5.7	11.1	17.8	117.1	27.8	539	552	583	621	677	780	832	934	718	3.7
CPC	0.805	0.63	9.3	0.981	16.0	2.10	44.6	40.8	10.3	3.4	11.0	65.0	25.2	538	554	590	637	706	838	906	1047	757	3.5
LSCO	0.854	0.57	18.7	0.993	14.0	1.58	25.0	61.1	6.1	7.8	15.5	149.1	28.9	540	554	588	631	692	806	865	984	741	3.8
Prinos	0.875	3.71	20.3	1.108	32.8	9.14	12.6	50.6	6.8	30.0	38.8	550	69.2	538	555	595	645	718	858	930	1085	760	6.8
SGC	0.883	2.26	30.1	1.050	22.9	5.09	15.0	55.9	7.3	21.8	28.4	451	58.4	540	564	619	689	789	981	1084	1319	891	5.9
Oryx	0.9156	4.209	37.4	1.089	29.4	8.01	13.3	50.1	5.7	30.9	39.6	714.0	84.8	537	571	653	764	931	1277	1473	1964	1130	8.3
Okwuibome	0.868	0.20	6.9	0.975	12.9	0.50	31.7	56.0	10.5	1.7	8.2	60.0	23.3	540	549	571	601	643	721	758	818	671	3.2
Boscan	1.002	5.50	63.1	1.078	27.8	6.00	15.1	44.5	5.3	35.2	41.0	1003.0	115.0	542	588	689	812	982	1295	1459	1841	1330	8.7
RasGharib	0.926	3.44	40.2	1.059	25.1	5.60	14.7	49.7	5.6	26.0	34.9	610.0	75.8	540	567	628	706	814	1020	1128	1383	940	6.4
Varandey	0.850	0.63	14.9	0.990	15.1	1.70	33.5	47.6	11.3	7.6	13.5	103.0	43.8	539	552	582	621	677	783	837	942	717	3.7
Albania	1.001	5.64	48.2	1.094	31.4	8.70	10.0	52.9	6.3	37.7	49.7	680.0	92.2	540	572	645	732	850	1061	1166	1388	1017	7.9
Tempa Rossa	0.940	5.35	37.6	1.120	34.3	9.3	2.2	48.4	12.6	36.8	46.8	759.5	100.0	540	568	630	708	816	1021	1129	1383	931	8.2
Forties	0.817	0.68	11.9	0.990	14.8	2.5	28.7	60.3	3.8	7.2	9.8	140.0	28.9	541	557	594	643	716	858	932	1081	772	3.8
Rhemoura	0.865	0.75	20.2	1.041	23.7	1.8	19.7	49.8	7.3	23.2	31.3	255	51.1	538	555	593	642	713	846	916	1063	766	5.2
Cheleken	0.847	0.40	16.6	0.974	12.3	1.2	34.2	51.8	8.2	5.8	12.5	81	35.7	541	556	589	632	694	810	869	989	745	3.2
Arab Light	0.858	1.89	22.9	1.029	18.7	4.9	15.9	64.7	7.3	12.1	18.8	192	32.3	540	558	597	647	716	843	908	1049	778	4.9
Azeri Light	0.848	0.20	14.8	0.967	9.5	0.5	40.2	50.1	8.4	1.4	5.4	77	30.2	539	553	585	627	686	799	856	971	731	3.0
Aseng	0.874	0.26	13.8	0.984	14.2	0.6	32.7	48.5	15.2	3.7	10.0	77	28.0	541	549	569	595	630	694	723	776	658	3.4
Buzachi	0.907	1.57	32.7	1.007	16.0	3.1	25.0	67.4	5.8	1.8	6.1	207	38.0	542	562	610	672	761	934	1025	1227	848	4.4
KBT	0.876	2.91	25.8	1.067	26.9	6.4	12.3	53.6	9.2	24.9	32.4	400	62.4	540	560	607	665	749	907	990	1174	821	6.2

* Note: the kinematic viscosity shown in Table 1 concerned the kinematic viscosity of the 70% *SRVR*/30% *FCC HCO* blend.**Table 3.** Physicochemical properties of hydrocracked vacuum residues (H-Oil VTBs).

No.	H-Oil Conv., wt. %	H-Oil VTB SG	H-Oil VTB CCR	Sat., wt. %	Aro, wt. %	Res, wt. %	C ₇ -Asp, wt. %	C ₅ -Asp, wt. %	Kin. Vis., mm ² /s	Soft. Point, °C	IBP	10%	30%	50%	70%	90%	95%	FBP	MW	ARI
1	75	1.006	21.8	26.4	53.7	9.7	10.1	21.0	90.7	37.8	541	551	573	598	629	679	702	744	663	4.0
2	69	1.011	22.6	25.6	56.4	11.2	6.8	26.4	106.7	38.4	541	552	574	599	631	680	703	744	666	4.1
3	70	1.021	23.4	23.8	48.9	11.9	15.4	26.0	112.8	37.5	541	551	573	597	628	677	700	741	661	4.4
4	75	1.021	24.1	23.9	48.8	12.8	14.5	27.0	103.1	38.1	541	551	574	599	631	683	706	750	665	4.4
5	65	1.025	23.6	23.3	51.2	9.4	16.1	23.6	103.7	41.3	539	550	572	597	629	681	704	749	661	4.4
6	64	1.015	22.1	24.8	49.0	10.9	15.3	24.9	117.2	37.9	539	550	572	596	628	677	700	742	660	4.2
7	59	1.002	19.1	27.4	48.6	13.2	10.8	25.5	89.2	27.6	540	551	574	600	631	682	704	748	668	3.9
8	68	1.026	23.6	23.1	48.7	11.8	16.4	26.0	116.4	41.0	539	550	572	598	631	684	708	753	662	4.5
9	73	1.036	24.0	21.7	49.9	13.9	14.5	28.5	114.7	36.0	540	550	572	597	629	681	705	748	659	4.7
10	67	1.029	23.1	22.6	47.5	15.2	14.7	28.6	103.3	38.5	540	552	577	604	638	691	715	763	676	4.6

Table 3. Cont.

No.	H-Oil Conv., wt.%	H-Oil VTB SG	H-Oil VTB CCR	Sat., wt.%	Aro, wt.%	Res, wt.%	C ₇ -Asp, wt.%	C ₅ -Asp, wt.%	Kin. Vis., mm ² /s	Soft. Point, °C	IBP	10%	30%	50%	70%	90%	95%	FBP	MW	ARI
11	61.3	1.009	22.5	25.9	43.1	12.8	18.2	28.9	89.6	40.7	539	553	581	610	645	700	724	774	691	4.1
12	62.0	1.016	22.5	24.6	48.8	15.9	10.7	27.7	106.6	37.4	541	553	579	609	645	703	730	783	687	4.3
13	55.3	0.9860	17.9	31.1	43.3	9.8	15.7	24.5	78.4	26.7	541	552	575	601	633	684	706	749	671	3.5
14	72.3	1.027	24.7	22.9	48.7	10.7	17.7	27.4	89.6	39.4	541	554	580	609	643	699	724	773	686	4.6
15	67.4	1.020	23.3	23.9	51.2	8.5	16.4	25.4	96.5	33.5	540	551	574	599	631	682	704	748	665	4.3
16	65.8	1.013	22.4	25.2	49.9	14.7	10.2	26.3	90.2	33.5	539	550	573	598	630	679	702	744	664	4.2
17	64.9	1.018	23.3	24.3	48.7	11.5	15.4	24.4	74.2	28.0	540	551	575	601	634	684	707	751	670	4.3
18	72.5	1.034	25.5	22.0	50.7	10.2	17.2	25.8	107	40.85	541	551	574	599	632	686	710	756	664	4.7
19	75.3	1.042	25.5	21.0	49.8	10.7	18.5	28.5	111.7	44.6	541	551	573	598	632	688	713	761	662	4.8
20	81.2	1.056	28.2	19.6	54.2	6.2	20.0	23.1	113.9	50.9	539	549	570	594	626	678	701	744	651	5.1
21	71.6	1.030	24.4	22.5	50.8	5.4	21.3	26.0	109.9	55.8	540	550	570	594	624	673	694	734	653	4.5
22	74.3	1.059	28.8	19.3	52.0	5.9	22.8	27.5	147.0	56.3	541	550	571	595	627	678	702	744	653	5.2
23	71.7	1.036	25.7	21.6	52.4	4.5	21.4	24.2	119.7	44.7	541	551	573	599	634	691	718	767	664	4.7
24	75.7	1.050	27.6	20.1	51.8	15.2	12.9	29.8	135.7	51.1	541	551	572	596	628	679	702	744	656	5.0
25	67.0	1.009	22.2	25.9	50.8	8.7	14.6	21.9	95.5	37.8	540	551	573	598	630	680	702	745	664	4.1
26	68.9	1.022	22.4	23.6	51.8	8.2	16.4	24.0	97.0	38.5	539	550	572	598	630	683	706	751	663	4.4
27	87.5	1.148	45.6	4.0	6.3	22.7	67.0	91.0	397.8	116.0	540	552	577	605	640	694	719	768	656	6.9
28	90.1	1.103	38	16.6	39.1	12.9	31.4	44.1	266.5	76	540	549	569	593	624	675	698	737	640	6.0
29	93.2	1.094	35.0	17.0	34.9	16.1	32.0	47.1	202.8	72.8	541	550	569	591	622	671	693	729	638	5.8
30	93.1	1.125	43.7	15.8	24.1	13.4	46.7	53.9	385.8	77.8	541	550	569	591	621	671	693	729	632	6.3
31	93	1.098	33.9	16.8	36.8	10.9	35.5	45.4	203.6	63.5	539	547	567	590	620	668	690	728	634	5.9
32	83.9	1.136	38.95	15.5	40.4	13.4	30.7	42.9	232.3	75.9	540	550	570	594	625	676	698	737	635	6.6
33	83.6	1.122	38.26	15.8	45.0	11.9	27.3	38.6	341.9	74.2	541	549	567	589	617	664	685	718	627	6

Saturate, aromatic, resin, and asphaltene (SARA) analysis of the studied vacuum residual oils was performed in accordance with the procedure described in [41]. The content of C₅- and C₇-asphaltenes was measured in accordance with the procedure described in [42].

Viscosity of the blends of studied 63 vacuum residues with fluid catalytic cracking heavy cycle oil at a ratio of 70% VR/30% FCC HCO was measured according to ASTM D1665 (Engler specific viscosity of tar products) at 80 °C. The properties of the FCC HCO were as follows: density at 15 °C = 1.000 g/cm³; high-temperature simulated distillation (HTSD), ASTM D7169): (evaporate, % = boiling point, °C) IBP = 241 °C; 10 wt.% = 272 °C; 30 wt.% = 297 °C; 50 wt.% = 316 °C; 70 wt.% = 337 °C; 90 wt.% = 367 °C; 95 wt.% = 382 °C; FBP = 431 °C, kin. viscosity at 80 °C = 3.25 mm²/s.

Conversion of the Engler specific viscosity in kinematic viscosity was performed as follows [43]:

$$Kin. vis. = 7.41 Engler\ specific\ viscosity \quad (1)$$

where *Kin. vis.* = kinematic viscosity, mm²/s; and *Engler specific viscosity* = Engler specific viscosity, °E.

The softening points (ring and ball) of the SRVRs and the H-Oil VTBs were measured according to BDS (Bulgarian standard) EN 1427 [44].

The distillation characteristics of the SRVRs were estimated on the basis of the distillation characteristics of the atmospheric residues and the use of Riazi's boiling point distribution model, as shown in Equation (2):

$$\frac{T_i - T_0}{T_0} = \left[\frac{A}{B} \ln \left(\frac{1}{1 - x_i} \right) \right]^{\frac{1}{B}} \quad (2)$$

where T_i is absolute boiling point (T_b), in K; x_i is the cumulative weight fraction; T_0 is the boiling point at $x_i = 0$; and A and B are boiling point distribution model parameters. During the estimation, T_0 was the fitting parameter that provided the best agreement between measured boiling points and those estimated by Equation (2).

The distillation characteristics of the VRs were extrapolated using the obtained three parameters of Equation (2): A , B , and T_0 . Table S1 presents the data from the ASTM D 5236 physical vacuum distillation of the atmospheric residues of the studied 30 crude oils. It also contains data on the values of the Riazi's distribution model parameters A and B ; T_0 ; and the average absolute deviation in boiling point prediction of the measured evaporates. Table S2 contains data for the high-temperature simulated distillation (HTSD, ASTM D 7169) of some of the SRVRs. The H-Oil VTBs' distillation characteristics were determined by application of the Riazi's boiling point distribution model to the HTSD of H-Oil atmospheric tower bottoms (ATBs). The HTSD characteristics of the 33 H-Oil ATBs are presented in Table S3. The physical vacuum distillation standard ASTM D 5236 was applied twice to two H-Oil ATB samples. Unfortunately, due to blocking of impulse lines of the ASTM D 5236 distillation apparatus with waxes, the apparatus controlling unit frequently experienced operational issues. For that reason, the measurement of the H-Oil ATB distillation characteristics by physical vacuum distillation was practically impossible. The results of the two H-Oil ATB samples analyzed using ASTM D 5236, along with application of Riazi's boiling point distillation to these distillation characteristic results, are summarized in Table S4. Table S4 also presents a comparison between the distillation characteristics of the two H-Oil VTBs extrapolated by Riazi's distribution model applied to the data of the physical vacuum distillation (ASTM D 5236) and of the gas chromatographic HTSD (ASTM D 7169).

The VR molecular weight was estimated by the use of the correlation developed by Linan et al. for heavy oils [27], and is shown as Equation (3):

$$M_w = 284.75 [\exp(0.00322(ABP + 273.15))] [\exp(-2.52SG)] \times (ABP + 273.15)^{0.083} SG^{2.44} \quad (3)$$

where M_w = molecular weight of the vacuum residue, g/mol; ABP = average boiling point, $ABP = \frac{(T_{10\%} + T_{30\%} + T_{50\%} + T_{70\%} + T_{90\%})}{5}$ °%; $T_{30\%}$, $T_{50\%}$, $T_{70\%}$, and $T_{90\%}$ are the temperatures of the evaporate at 10, 30, 50, 70, and 90% respectively, in K; and SG = specific gravity.

The molecular weight of the studied $SRVRs$ was estimated on the basis of the ABP obtained from the Riazi's boiling point distribution model applied to the data of the physical distillation (ASTM D 5236) of the atmospheric residue and extrapolated for the $SRVRs$. Due to observed cokelike material deposition in the gas chromatographic column inlet during vacuum residue HTSD analysis and the reported column cracking described in [30,31], we decided not to use the HTSD data for calculation of the $SRVRs$ ' molecular weight.

The aromatic ring index (ARI), developed by Abutaqiya et al. [45,46], is an indicator of the number of condensed aromatic rings in the molecular structure of the vacuum residues, and is estimated by Equations (4) and (5):

$$ARI = f(MW, F_{RI}) = \frac{2\left[\frac{MW}{F_{RI}} - (3.5149MW + 73.1858)\right]}{(3.5074MW - 91.972 - (3.5149MW + 73.1858))} \quad (4)$$

where MW = molecular weight of the vacuum residues, in g/mol; and F_{RI} = function of refractive index.

$$F_{RI} = \frac{n_{D20}^2 - 1}{n_{D20}^2 + 2} \quad (5)$$

where n_{D20} = refractive index at 20 °C.

The refractive index of the studied vacuum residues was estimated by the correlation developed by Stratiev et al. [47], and is shown as Equation (6):

$$RI = 0.702091d_{15} - 0.00011T_{50} + 0.91493 \quad (6)$$

The following statistical parameters were employed to evaluate the different models of the primary and secondary vacuum residues' softening points and viscosities [48]:

$$\text{Relative error (E)} : E = \left(\frac{v_{exp} - v_{calc}}{v_{exp}} \right) \times 100 \quad (7)$$

$$AARE = \frac{1}{n} \sum_{i=1}^n \left| \frac{v_{exp} - v_{calc}}{v_{exp}} \right| \times 100 \quad (8)$$

$$\text{Standard error (SE)} : SE = \left(\sum \left(\frac{(v_{exp} - v_{calc})^2}{n} \right) \right)^{\frac{1}{2}}, \quad (9)$$

$$\text{Relative standard error (RSE)} : RSE = \frac{SE}{\text{mean of the sample}} \times 100, \quad (10)$$

$$\text{Sum of square errors (SSE)} : SSE = \sum \frac{1}{v_{exp}^2} (v_{exp} - v_{calc})^2 \quad (11)$$

$$\text{Residual (R)} : R = v_{exp} - v_{calc}, \quad (12)$$

$$\text{Relative error (RE)} : RE = \left(\sum \left(\frac{v_{exp} - v_{calc}}{v_{exp}} \right) \right) \times 100. \quad (13)$$

The Akaike information criterion (AIC) and Bayesian information criterion (BIC) were found to be capable of estimating the relative quality of a statistical method, and thus are able to provide the means for model selection [48,49] when several models are available. The estimations of AIC and BIC for the methods developed in this study are summarized below.

Akaike and Bayesian Information Criteria:

Consider the obtained errors $\{\epsilon_1, \dots, \epsilon_n\}$ as independent random samples from a density function $f(\epsilon_i | \theta)$, and supposing normal distribution of errors:

$$f(x|\theta) = f(x|\{\mu, \sigma\}) = \frac{1}{\sigma\sqrt{2\pi}} \exp\left(-\frac{1}{2}\left(\frac{x-\mu}{\sigma}\right)^2\right). \quad (14)$$

Then, by the definition of the likelihood function:

$$L(\theta) = \prod_{i=1}^n f(\epsilon_i|\theta) = \prod_{i=1}^n \frac{1}{\sigma\sqrt{2\pi}} \exp\left(-\frac{1}{2}\left(\frac{\epsilon_i-\mu}{\sigma}\right)^2\right). \quad (15)$$

The function L has a maximum if:

$$\mu = \hat{\mu} = \frac{1}{n} \sum_{i=1}^n \epsilon_i \text{ and } \sigma^2 = \hat{\sigma}^2 = \frac{1}{n} \sum_{i=1}^n (\epsilon_i - \hat{\mu})^2. \quad (16)$$

The Akaike information criterion (AIC) determines the relative information value of the model using the maximum likelihood value $\ln(L(\hat{\theta}))$, $\hat{\theta} = \{\hat{\mu}, \hat{\sigma}\}$, and the number of parameters:

$$\text{AIC} = 2 \times [\text{number of parameters}] - 2 \times \ln(L(\hat{\theta})).$$

The Bayesian information criterion is defined by:

$$\text{BIC} = [\text{number of parameters}] \times \ln([\text{number of data points}]) - 2 \times \ln(L(\hat{\theta})). \quad (17)$$

3. Results

3.1. Relations of the Vacuum Residue Properties to Viscosity and Softening Point

Table 4 summarizes the range of variation in the properties of the straight-run vacuum residual oils and the hydrocracked vacuum residual oils (H-Oil VTBs) under study. The range of variation was obtained by statistical analysis of the data in the Supplementary Material.

Table 4. Range of variation in SRVR and H-Oil VTB properties.

	SRVR		H-Oil VTB	
	Min.	Max	Min.	Max
SG	0.967	1.120	0.986	1.148
Conradson carbon content, wt.%	9.5	34.3	17.9	45.6
Saturates, wt.%	2.2	44.6	4.0	31.1
Aromatics, wt.%	40.8	73.5	6.3	56.4
Resins, wt.%	3.8	15.2	4.5	22.7
C ₇ -asphaltenes, wt.%	1.4	37.7	6.8	67.0
C ₅ -asphaltenes, wt.%	5.4	49.7	21.0	91.0
Molecular weight, g/mol	658	1330	627	691
Kin. viscosity of the blends of 70% VR/30% FCCHCO, mm ² /s	60	1003	74	398
Softening point, °C	23.3	115	27	116
Aromatic ring index	3.0	8.7	3.5	6.9

It was evident from these data that the range of variation in the physicochemical properties of the studied SRVROs and H-Oil VTBs was rather wide. Therefore, the data could be considered representative enough for the purpose of the investigation of the vacuum residue properties' relations. It was also observed in the data in Table 3 that the molecular weight of the SRVRs estimated by Equation (3) and using the average boiling point extrapolated by Riazi's distribution model was within the range of variation in molecular weights reported in Table 1. It was also within the range of variation in vacuum residue molecular weights (variation between 677 and 1265 g/mol) reported by van den Berg et al. [50] and determined by vapor pressure osmometry (VPO) for 11 crude

oils comprising extra light to heavy crude oils. Therefore, one may conclude that the procedure applied in this work for determination of vacuum residue molecular weight by the use of Equation (3) and Riazi's boiling point distribution model applied to the atmospheric residue distillation data presented consistent values. The data in Table 3 also showed that the molecular weights of the H-Oil VTBs varied in a narrow range, around 660 g/mol, which was much lower than the molecular weight of the typical LNB H-Oil VR hydrocracker Urals vacuum residue feed, about 800 g/mol. This was also consistent with the molecular weight reduction during VR hydrocracking, a result of the cracking of the aliphatic moieties of the VR feed components, leading to a hydrocracked vacuum residue with a lower molecular weight [51].

Intercriteria analysis (*ICrA*) was employed to determine statistically significant relations between the different properties of the primary and secondary vacuum residues. More information concerning the application of *ICrA* can be found in our recent studies [28,29]. *ICrA* defines the relations between the studied criteria (parameters) in terms of intuitionistic fuzzy pairs (μ, ν) [28,29]. Depending on the values of μ, ν seen in a pair, positive consonance, negative consonance, and dissonance between any pair of criteria (parameters) can be defined. Values of $\mu = 0.75\text{--}1.00$ and $\nu = 0.00\text{--}0.25$ denote a statistically meaningful positive relation, where the strong positive consonance is exhibited at values of $\mu = 0.95\text{--}1.00, \nu = 0.00\text{--}0.05$; and the weak positive consonance is exhibited at values of $\mu = 0.75\text{--}0.85, \nu = 0.15\text{--}0.25$. The values of negative consonance with $\mu = 0.00\text{--}0.25$ and $\nu = 0.75\text{--}1.05$ represent a statistically meaningful negative relation, where the strong negative consonance exhibits values of $\mu = 0.00\text{--}0.05, \nu = 0.95\text{--}1.00$; and the weak negative consonance exhibits values of $\mu = 0.15\text{--}0.25, \nu = 0.15\text{--}0.25$. All other cases are characterized as dissonance [28,29].

Tables 5 and 6 present the statistically meaningful relations quantified by the μ - and ν -values for the *ICrA* of the evaluated SRVRs.

Table 5. The μ -values for the *ICrA* evaluation of relations between properties of the studied SRVRs.

	Crude d_{15}	Crude S	VR	VR SG	VR CCR	VR S	Sat	Aro	Res	C7-Asp	C5-Asp	VIS	SP	T50%	MW	ARI
Crude d_{15}	1.000	0.777	0.903	0.756	0.766	0.708	0.267	0.467	0.453	0.789	0.777	0.768	0.766	0.805	0.800	0.784
Crude S	0.777	1.000	0.828	0.885	0.887	0.922	0.191	0.490	0.359	0.885	0.885	0.874	0.812	0.855	0.846	0.917
VR	0.903	0.828	1.000	0.772	0.763	0.754	0.271	0.508	0.384	0.818	0.807	0.807	0.777	0.878	0.878	0.809
VR SG	0.756	0.885	0.772	1.000	0.924	0.899	0.154	0.476	0.425	0.897	0.881	0.876	0.814	0.789	0.775	0.929
VR CCR	0.766	0.887	0.763	0.924	1.000	0.885	0.195	0.451	0.439	0.901	0.899	0.864	0.805	0.775	0.770	0.894
VR S	0.708	0.922	0.754	0.899	0.885	1.000	0.161	0.520	0.386	0.835	0.832	0.823	0.768	0.812	0.798	0.881
Sat	0.267	0.191	0.271	0.154	0.195	0.161	1.000	0.354	0.554	0.244	0.251	0.246	0.303	0.248	0.258	0.168
Aro	0.467	0.490	0.508	0.476	0.451	0.520	0.354	1.000	0.324	0.414	0.421	0.439	0.368	0.533	0.538	0.469
Res	0.453	0.359	0.384	0.425	0.439	0.386	0.554	0.324	1.000	0.421	0.409	0.398	0.483	0.352	0.349	0.384
C7-asp	0.789	0.885	0.818	0.897	0.901	0.835	0.244	0.414	0.421	1.000	0.966	0.947	0.858	0.802	0.798	0.890
C5-asp	0.777	0.885	0.807	0.881	0.899	0.832	0.251	0.421	0.409	0.966	1.000	0.926	0.851	0.795	0.791	0.885
VIS	0.768	0.874	0.807	0.876	0.864	0.823	0.246	0.439	0.398	0.947	0.926	1.000	0.860	0.828	0.823	0.892
SP	0.766	0.812	0.777	0.814	0.805	0.768	0.303	0.368	0.483	0.858	0.851	0.860	1.000	0.761	0.754	0.830
T50%	0.805	0.855	0.878	0.789	0.775	0.812	0.248	0.533	0.352	0.802	0.795	0.828	0.761	1.000	0.984	0.846
MW	0.800	0.846	0.878	0.775	0.770	0.798	0.258	0.538	0.349	0.798	0.791	0.823	0.754	0.984	1.000	0.832
ARI	0.784	0.917	0.809	0.929	0.894	0.881	0.168	0.469	0.384	0.890	0.885	0.892	0.830	0.846	0.832	1.000

Note: Green color means a statistically meaningful positive relation; red color implies a statistically meaningful negative relation. The intensity of the color designates the strength of the relation: the higher the color intensity, the higher the strength of the relation. Yellow color denotes dissonance.

Table 6. The ν -values for the $ICrA$ evaluation of relations between properties of the studied $SRVRs$.

	Crude d_{15}	Crude S	VR	VR SG	VR CCR	VR S	Sat	Aro	Res	C7-Asp	C5-Asp	VIS	SP	T50%	MW	ARI
Crude d_{15}	0.000	0.212	0.090	0.223	0.228	0.278	0.717	0.526	0.524	0.207	0.218	0.228	0.228	0.186	0.195	0.193
Crude S	0.212	0.000	0.163	0.092	0.103	0.067	0.791	0.501	0.616	0.108	0.108	0.120	0.179	0.133	0.147	0.058
VR	0.090	0.163	0.000	0.209	0.232	0.235	0.715	0.487	0.595	0.179	0.191	0.191	0.218	0.115	0.120	0.170
VR SG 15	0.223	0.092	0.209	0.000	0.058	0.081	0.818	0.506	0.540	0.087	0.103	0.108	0.168	0.195	0.209	0.046
VR CCR	0.228	0.103	0.232	0.058	0.000	0.103	0.791	0.545	0.540	0.097	0.099	0.133	0.191	0.218	0.228	0.085
VR S	0.278	0.067	0.235	0.081	0.103	0.000	0.818	0.469	0.586	0.156	0.159	0.168	0.221	0.179	0.193	0.097
Sat	0.717	0.791	0.715	0.818	0.791	0.818	0.000	0.632	0.416	0.745	0.738	0.743	0.683	0.736	0.731	0.802
Aro	0.526	0.501	0.487	0.506	0.545	0.469	0.632	0.000	0.655	0.584	0.577	0.559	0.628	0.460	0.460	0.510
Res	0.524	0.616	0.595	0.540	0.540	0.586	0.416	0.655	0.000	0.561	0.572	0.584	0.497	0.625	0.632	0.579
C7-asp	0.207	0.108	0.179	0.087	0.097	0.156	0.745	0.584	0.561	0.000	0.035	0.053	0.140	0.193	0.202	0.092
C5-asp	0.218	0.108	0.191	0.103	0.099	0.159	0.738	0.577	0.572	0.035	0.000	0.074	0.147	0.200	0.209	0.097
VIS	0.228	0.120	0.191	0.108	0.133	0.168	0.743	0.559	0.584	0.053	0.074	0.000	0.138	0.168	0.177	0.090
SP	0.228	0.179	0.218	0.168	0.191	0.221	0.683	0.628	0.497	0.140	0.147	0.138	0.000	0.232	0.244	0.154
T50%	0.186	0.133	0.115	0.195	0.218	0.179	0.736	0.460	0.625	0.193	0.200	0.168	0.232	0.000	0.012	0.136
MW	0.195	0.147	0.120	0.209	0.228	0.193	0.731	0.460	0.632	0.202	0.209	0.177	0.244	0.012	0.000	0.149
ARI	0.193	0.058	0.170	0.046	0.085	0.097	0.802	0.510	0.579	0.092	0.097	0.090	0.154	0.136	0.149	0.000

Note: Green color means a statistically meaningful positive relation; red color implies a statistically meaningful negative relation. The intensity of the color designates the strength of the relation: the higher the color intensity, the higher the strength of the relation. Yellow color denotes dissonance.

It was evident from these data that the viscosities of the $SRVRs$ had statistically meaningful relations of the crude density and sulfur content with the vacuum residue content in the crude oil and the vacuum residue properties of density, Conradson carbon content, asphaltene content, average boiling point, molecular weight, and aromatic ring index (ARI). Among these, the strongest was the relation with asphaltene content and ARI . The same $SRVR$ properties had statistically meaningful relations to the softening point, and the asphaltene content had the strongest relation to the $SRVR$ softening point.

Tables 7 and 8 present the statistically meaningful relations quantified by the μ - and ν -values for the $ICrA$ of the evaluated H-Oil $VTBs$.

Table 7. The μ -values for the $ICrA$ evaluation of relations between properties of the studied H-Oil $VTBs$.

	H-Oil Conv.	VTB d_{15}	VTB CCR	Sat	Aro	Res	VTB C7-Asp	VTB C5-Asp	VTB VIS	SP	T50%	MW	ARI
H-Oil Conv.	1.000	0.839	0.845	0.155	0.441	0.544	0.727	0.712	0.790	0.796	0.231	0.195	0.826
VTB d_{15}	0.839	1.000	0.926	0.002	0.392	0.553	0.803	0.729	0.856	0.858	0.241	0.189	0.966
VTB CCR	0.845	0.926	1.000	0.061	0.394	0.547	0.797	0.733	0.831	0.860	0.267	0.214	0.911
Sat	0.155	0.002	0.061	1.000	0.583	0.434	0.180	0.261	0.136	0.133	0.691	0.786	0.006
Aro	0.441	0.392	0.394	0.583	1.000	0.252	0.311	0.222	0.415	0.403	0.449	0.508	0.367
Res	0.544	0.553	0.547	0.434	0.252	1.000	0.447	0.741	0.566	0.515	0.492	0.472	0.549
VTB C7-asp	0.727	0.803	0.797	0.180	0.311	0.447	1.000	0.674	0.731	0.811	0.313	0.280	0.780
VTB C5-asp	0.712	0.729	0.733	0.261	0.222	0.741	0.674	1.000	0.716	0.716	0.386	0.367	0.727
VTB VIS	0.790	0.856	0.831	0.136	0.415	0.566	0.731	0.716	1.000	0.833	0.201	0.163	0.833
SP	0.796	0.858	0.860	0.133	0.403	0.515	0.811	0.716	0.833	1.000	0.256	0.216	0.835
T50%	0.231	0.241	0.267	0.691	0.449	0.492	0.313	0.386	0.201	0.256	1.000	0.890	0.244
MW	0.195	0.189	0.214	0.786	0.508	0.472	0.280	0.367	0.163	0.216	0.890	1.000	0.193
ARI	0.826	0.966	0.911	0.006	0.367	0.549	0.780	0.727	0.833	0.835	0.244	0.193	1.000

Note: Green color means a statistically meaningful positive relation; red color implies a statistically meaningful negative relation. The intensity of the color designates the strength of the relation: the higher the color intensity, the higher the strength of the relation. Yellow color denotes dissonance.

Table 8. The v -values for the $ICrA$ evaluation of relations between properties of the studied H-Oil VTBs.

	H-Oil Conv.	VTB d_{15}	VTB CCR	Sat	Aro	Res	VTB C7-Asp	VTB C5-Asp	VTB VIS	SP	T50%	MW	ARI
H-Oil Conv.	0.000	0.152	0.142	0.835	0.540	0.441	0.260	0.277	0.205	0.195	0.699	0.778	0.135
VTB d_{15}	0.152	0.000	0.059	0.991	0.587	0.430	0.182	0.258	0.136	0.131	0.688	0.782	0.004
VTB CCR	0.142	0.059	0.000	0.924	0.581	0.432	0.184	0.250	0.157	0.125	0.661	0.754	0.047
Sat	0.835	0.991	0.924	0.000	0.396	0.549	0.805	0.725	0.856	0.856	0.241	0.189	0.956
Aro	0.540	0.587	0.581	0.396	0.000	0.722	0.665	0.756	0.568	0.576	0.470	0.455	0.581
Res	0.441	0.430	0.432	0.549	0.722	0.000	0.532	0.241	0.421	0.468	0.430	0.494	0.403
VTB C7-asp	0.260	0.182	0.184	0.805	0.665	0.532	0.000	0.309	0.258	0.174	0.616	0.688	0.174
VTB C5-asp	0.277	0.258	0.250	0.725	0.756	0.241	0.309	0.000	0.275	0.271	0.540	0.602	0.233
VTB VIS	0.205	0.136	0.157	0.856	0.568	0.421	0.258	0.275	0.000	0.159	0.731	0.813	0.129
SP	0.195	0.131	0.125	0.856	0.576	0.468	0.174	0.271	0.159	0.000	0.676	0.756	0.123
T50%	0.699	0.688	0.661	0.241	0.470	0.430	0.616	0.540	0.731	0.676	0.000	0.044	0.661
MW	0.778	0.782	0.754	0.189	0.455	0.494	0.688	0.602	0.813	0.756	0.044	0.000	0.756
ARI	0.135	0.004	0.047	0.956	0.581	0.403	0.174	0.233	0.129	0.123	0.661	0.756	0.000

Note: Green color means a statistically meaningful positive relation; red color implies a statistically meaningful negative relation. The intensity of the color designates the strength of the relation: the higher the color intensity, the higher the strength of the relation. Yellow color denotes dissonance.

These data showed that the H-Oil VTBs had statistically meaningful relations to the H-Oil conversion, and the H-Oil VTB properties of density, Conradson carbon content, saturate content, softening point, average boiling point, molecular weight, and ARI. The strongest were the relations with the density and saturate content. While the relation with density was positive, that with the saturate content was negative. Unlike the $SRVRs$, the H-Oil VTBs' viscosities increased with the decrease in molecular weight, which was evident from the negative consonances shown in Table 7. The reason for this difference between the $SRVRs$ and H-Oil VTBs concerning viscosity can be explained by the fact that during increasing H-Oil conversion, the H-Oil VTB molecular weight decreased, and simultaneously its aromaticity, expressed by density, and Conradson carbon content were augmented, which in turn led to increasing the H-Oil VTBs' viscosities. The same H-Oil VTB properties had statistically meaningful relations with the H-Oil VTB softening point. The strongest was the relation of the H-Oil VTB softening point to the Conradson carbon, which was positive, and to the saturate content, which was negative.

$ICrA$ allowed us not only to define the statistically meaningful relations between the properties of the primary and the secondary vacuum residues, but also to quantify the extent of similarities between the individual vacuum residues. Table 9 presents an illustration of the extent of the similarities between some of the individual $SRVRs$, as well as the complete dissimilarities between the $SRVRs$ and the H-Oil VTBs quantified by the $ICrA$ parameters of consonance and dissonance. Green color means a statistically meaningful positive relation; red color implies a statistically meaningful negative relation. The intensity of the color designates the strength of the relation: the higher the color intensity, the higher the strength of the relation. Yellow color denotes dissonance.

Table 9. The μ -values of the $ICrA$ evaluation of similarities between the individual $SRVRs$ and individual H-Oil VTBs.

	Urals	Arab Med	Arab Heavy	Val'Dagri	Basrah Light	Basrah Heavy	Kirkuk	Iranian Heavy	KEB	El Bourri
Urals	1.00	0.73	0.71	0.68	0.71	0.61	0.65	0.65	0.76	0.60
Arab Med	0.73	1.00	0.94	0.82	0.95	0.86	0.80	0.67	0.84	0.76
Arab Heavy	0.71	0.94	1.00	0.78	0.93	0.89	0.76	0.64	0.80	0.78
Val'Dagri	0.68	0.82	0.78	1.00	0.82	0.77	0.79	0.71	0.78	0.78
Basrah Light	0.71	0.95	0.93	0.82	1.00	0.86	0.82	0.69	0.85	0.80
Basrah Heavy	0.61	0.86	0.89	0.77	0.86	1.00	0.86	0.73	0.79	0.74
Kirkuk	0.65	0.80	0.76	0.79	0.82	0.86	1.00	0.85	0.85	0.69

Table 9. Cont.

	Urals	Arab Med	Arab Heavy	Val'Dagri	Basrah Light	Basrah Heavy	Kirkuk	Iranian Heavy	KEB	El Bouri
Iranian Heavy	0.65	0.67	0.64	0.71	0.69	0.73	0.85	1.00	0.80	0.56
KEB	0.76	0.84	0.80	0.78	0.85	0.79	0.85	0.80	1.00	0.67
El Bouri	0.60	0.76	0.78	0.78	0.80	0.74	0.69	0.56	0.67	1.00
CPC	0.86	0.69	0.65	0.66	0.65	0.54	0.56	0.54	0.69	0.69
LSCO	0.94	0.75	0.73	0.70	0.73	0.62	0.65	0.67	0.78	0.63
Prinos	0.42	0.59	0.63	0.69	0.61	0.74	0.73	0.74	0.59	0.59
SGC	0.75	0.84	0.80	0.71	0.84	0.86	0.90	0.84	0.89	0.64
Boscan	0.48	0.56	0.57	0.41	0.55	0.55	0.52	0.50	0.56	0.35
RasGharib	0.66	0.78	0.78	0.69	0.78	0.84	0.84	0.82	0.81	0.60
Varandey	0.83	0.61	0.59	0.63	0.59	0.51	0.54	0.61	0.63	0.61
Albanian crude	0.52	0.70	0.72	0.64	0.71	0.78	0.72	0.70	0.67	0.56
Tempa rossa	0.49	0.60	0.61	0.66	0.63	0.71	0.79	0.81	0.71	0.59
Forties	0.93	0.78	0.76	0.71	0.76	0.67	0.70	0.71	0.81	0.58
H-Oil Conv.75%	0.43	0.28	0.22	0.41	0.29	0.25	0.39	0.48	0.37	0.39
H-Oil Conv.58.5%	0.46	0.29	0.24	0.40	0.30	0.23	0.35	0.44	0.39	0.42
H-Oil Conv.67.5%	0.41	0.23	0.18	0.38	0.25	0.27	0.41	0.49	0.39	0.39
H-Oil Conv.64.9%	0.50	0.33	0.28	0.42	0.35	0.24	0.36	0.43	0.43	0.46
H-Oil Conv.93.2%	0.31	0.24	0.20	0.36	0.25	0.29	0.41	0.48	0.37	0.34
H-Oil Conv.83.6%	0.31	0.25	0.25	0.39	0.30	0.33	0.44	0.50	0.37	0.37

Note: Green color means a statistically meaningful positive relation; red color implies a statistically meaningful negative relation. The intensity of the color designates the strength of the relation: the higher the color intensity, the higher the strength of the relation. Yellow color denotes dissonance.

The data in Table 9 indicated a positive consonance between the SRVRs; for example, Urals had positive consonances of $\mu = 0.94$ with Light Siberian (LSCO) and $\mu = 0.93$ with Forties, while Arab Medium had a strong positive consonance of $\mu = 0.95$ with Basrah Light. Dissonance, and very rarely a negative consonance, were observed between the SRVRs; whereas between all SRVRs and all H-Oil VTBs, only negative consonances were registered. This implied that the physicochemical nature of the hydrocracked vacuum residues was substantially different from that of the SRVRs.

We concluded from the results of the ICrA that the SRVR properties of viscosity and softening point were affected in a different way than the other properties, and therefore their modeling should be performed separately.

3.2. Modeling Straight-Run Vacuum Residue and Hydrocracked Vacuum Residue Viscosity and Softening Point

Redelius and Soenen [52] proposed that the viscosity of bitumen and vacuum residue is determined by interactions between the molecules. Larger molecules, as well as large polyaromatic systems, result in higher interactions, and thus a higher viscosity [52]. This can explain why the molecular weight, which accounts for the size of the molecules, and the specific gravity (density), which accounts for the content of aromatics, [28,42] are the oil parameters that, along with the modified empirical model of Walther (Equation (18)) [53], can be used to properly predict oil viscosity. Another indirect estimate of molecular weight is the boiling point, which is roughly related to the molecular size [52]. Our recent studies on modeling the viscosities of gas oils [29,54] showed that the modified empirical model of Walther [53], in which two oil characteristics (average boiling point (ABP) and specific gravity) and Equation (18) can be used to properly predict oil viscosity:

$$Vis = e^{eaABP^b.SG^c + d} + f \quad (18)$$

where Vis = kinematic viscosity of gas oil at 80 °C, in mm^2/s ; ABP = average boiling point, in K; SG = specific gravity; and $a, b, c, d, e,$ and f = empirical coefficients estimated on the basis of experimental data and the use of the computer algebra system Maple (and the Global Optimization Toolbox). All computations were performed by the use of CAS Maple and NLPsolve with the modified Newton iterative method starting from the corresponding initial condition. The stop criteria was the absolute difference of two consecutive iterations

being less than or equal to 0.01. More details on the application of the CAS Maple and NLPsolve with the modified Newton iterative method and the benefit of its usage for oil viscosity modeling was given in our recent study [54].

The same model as that of Equation (18) was employed to simulate the viscosity of the blends of 70% SRVR/30% FCC HCO while employing data for 10 blends of 70% SRVR/30% FCC HCO from our earlier study [55] and 23 blends of 70% SRVR/30% FCC HCO shown in Table 1. The remaining seven blends of 70% SRVR/30% FCC HCO will be later used for verification of the models. Model 1 employed the SRVR characteristics of molecular weight (*MW*) and specific gravity (*SG*). Model 2 used the SRVR characteristics of molecular weight (*MW*) and *C*₇-asphaltene content. Model 3 applied the SRVR characteristics of *ABP* and *SG*. Another model to predict SRVR viscosity was developed by employing *MW* and *ARI* as input variables and the use of Equation (19):

$$VIS = \frac{ARI^a}{(\ln(\ln(b + MW)) - c)^d} + f, \quad a, b, c, d, f > 0. \quad (19)$$

Table 10 presents the values of the four estimated model parameters using the procedure described above.

Table 10. Values of the SRVR viscosity model parameters of Models 1–4.

Model Parameters	Model 1 (Equation (18)) (SRVR VIS)	Model 2 (Equation (18)) (SRVR VIS)	Model 3 (Equation (18)) (SRVR VIS)	Model 4 (Equation (19)) (SRVR VIS)
a	−5.00865	−8.05983	−10.99957	2.266
b	0.19482	0.24726	0.23653	3261.12086
c	0.91620	0.25887	0.37364	3.0125
d	3.10347	2.46841	3.99885	1
f	−132.76	41.3679	−287.281	−30

Table 11 summarizes the statistical analyses, showing the minimum error (min *E*), maximum error (*max E*), number of positive residuals (#*R*+) and negative residuals (#*R*−), range calculated by the difference between the highest positive residual (*HPR*) and the lowest negative residual (*LNR*), fitting parameters, Akaike information criterion (*AIC*), and Bayesian information criterion (*BIC*), which provided a sound evaluation of the three SRVR viscosity models. These data indicated that Model 2, which employed Equation (18) and the SRVR characteristics of *MW* and *C*₇-asphaltene content, was characterized by the lowest error, highest coefficient of determination *R*², and lowest *AIC* and *BIC*. This implied that Model 2 was the preferred model to simulate the SRVR viscosity.

Table 11. Statistical analysis of the four SRVR viscosity models.

	Model 1 (SRVR VIS)	Model 2 (SRVR VIS)	Model 3 (SRVR VIS)	Model 4 (SRVR VIS)
<i>Min E</i>	−83.4	−72.1	−82.3	−82.9
<i>Max E</i>	39.2	25.4	37.5	40.6
<i>RE</i>	192.0	−65.3	129.7	8237
<i>SE</i>	82.9	58.1	85.1	80.9
<i>RSE</i>	23.1	16.2	23.8	22.6
<i>SSE</i>	1.5	1.41	1.53	1.72
<i>AARE</i>	15.3	16.2	16.4	18.2
# <i>R</i> +	18	11	17	11
# <i>R</i> −	11	18	12	18
<i>HPR</i>	227	173.6	230.1	189

Table 11. *Cont.*

	Model 1 (SRVR VIS)	Model 2 (SRVR VIS)	Model 3 (SRVR VIS)	Model 4 (SRVR VIS)
LNR	101	−87.7	−57.2	−105
R ²	0.8929	0.9405	0.9078	0.8922
Slope	0.8768	0.9164	0.7878	0.8758
Intercept	11.8	19.2	38.7	18.5
AIC	8.4	7.0	8.5	15.9
BIC	12.6	11.2	12.7	20.3

The softening point as a physical property of bitumen and vacuum residue, as Redelius and Soenen explained in their study [52], is also a function of the interactions between the molecules. Therefore, one may expect that the softening point will depend on the same vacuum residue properties as viscosity does. Since Equation (18) did not provide a satisfactory modeling of SRVR softening point, another model equation was employed to simulate the SRVR softening point. It is shown as Equation (20):

$$SP = a \left(\frac{SG(C7_{asp}; CCR)^d}{\ln(\ln(b + MW)) - c} \right)^f + g, \quad a, b, d, f, g > 0. \quad (20)$$

Table 12 presents the values of the estimated model parameters for simulation of the SRVR softening point by Equation (20) through employment of the characteristics of molecular weight (*MW*) and specific gravity (*SG*)—Model 5 (*SP*); molecular weight (*MW*) and C₇-asphaltene content—Model 6 (*SP*); and molecular weight (*MW*) and Conradson carbon content (*CCR*)—Model 7 (*SP*). In Models 6 and 7, the C₇-asphaltene content and *CCR* took the place of *SG* in Equation (20).

Table 12. Values of the SRVR softening point model parameters of Models 5–7.

Model Parameters	Model 5 (SRVR SP)	Model 6 (SRVR SP)	Model 7 (SRVR SP)
a	0.999462	0.247470	0.021333
b	3273.077761	3272.091072	3273.035253
c	−1.797226	2.122597	1.330416
d	3.99998	2.15585	3.727435
f	2.991707	0.901634	0.688136
g	2.056976	25.747997	20.951802

Table 13 summarizes the statistical analyses, showing the minimum error (min *E*), maximum error (*max E*), number of positive residuals (#*R*+) and negative residuals (#*R*−), range calculated by the difference between the highest positive residual (*HPR*) and the lowest negative residual (*LNR*), fitting parameters, Akaike information criterion (*AIC*), and Bayesian information criterion (*BIC*), which provided a sound evaluation of the three SRVR softening-point models. It can be seen from the data in Table 12 that Model 5 exhibited the lowest *AIC*, *BIC*, *AARE*, and *SSE*, and therefore was considered as the best model to simulate the SRVR softening point. It seemed that the C₇-asphaltene content was a better descriptor of the SRVR softening point than the *SG* and *CCR*.

Table 13. Statistical analysis of the three SRVR softening-point models.

	Model 5 (SRVR SP)	Model 6 (SRVR SP)	Model 7 (SRVR SP)
Min E	−53.2	−19.0	−32.1
Max E	61.2	56.0	55.4
RE	105.6	161.2	108.9
SE	0.7	1.0	0.9
RSE	1.3	1.8	1.6
SSE	1.30	0.70	0.90
AARE	15.7	11.9	13.6
#R+	15	15	14
#R−	8	8	9
HPR	48.5	35.3	48.1
LNR	−36.8	−6.5	−22.2
R ²	0.5821	0.8362	0.665
Slope	0.7862	0.8518	0.7165
Intercept	8.5	3.5	11.4
AIC	14.9	−1.4	7.0
BIC	13.3	0.4	8.6

The viscosity of the blends of 70% H-Oil VTBs/30% FCC HCO was found to be best modeled by the exponential dependence on the H-Oil VTB Conradson carbon content (CCR) using Equation (21):

$$HOil\ VT B\ VIS = 25.021 \times \exp(0.0603 \times VT B\ CCR) \quad R^2 = 0.937; \%AAD = 8.5 \quad (21)$$

where *HOil VT B VIS* = viscosity of the blends of 70% H-Oil VTBs/30% FCC HCO at 80 °C, in mm²/s; and *VT B CCR* = H-Oil VT B Conradson carbon content, in wt.%.

The softening point of the H-Oil VT B was also found to be best modeled by the exponential dependence on the H-Oil VT B Conradson carbon content (CCR) using Equation (22):

$$HOil\ VT B\ SP = 13.093 \times \exp(0.0461 * VT B\ CCR) \quad R^2 = 0.891; AARE = 8.2\% \quad (22)$$

where *HOil VT B SP* = softening point of H-Oil VTBs, in °C.

Unlike the SRVRs, the H-Oil VTBs' rheological properties of viscosity and softening point did not increase with the molecular weight (MW) augmentation. The reason was that the H-Oil VT B CCR was enhanced with conversion magnification, as evident from the data in Table 6, while the MW decreased with conversion increment. This can be explained by the chemistry of the vacuum residue hydrocracking. With conversion enhancement, the aromaticity and CCR of the H-Oil VTBs increased due to cleavage of the aliphatic moieties attached to the aromatic rings, which in turn led to a VT B product with a lower molecular weight. As observed from Equations (21) and (22), the CCR magnification had a positive effect on both the viscosity and softening-point enhancement.

3.3. Validation of the Developed Models to Simulate Viscosities and Softening Points of SRVRs and H-Oil VTBs

The empirical models developed to predict SRVR viscosity (Models 1–4) were developed on the basis of data for 10 SRVRs taken from our earlier study [55] and 19 data sets taken from Table 1. The other 11 data sets in Table 2 were used to validate the prediction abilities of Models 1–4 to correctly predict the viscosity of the blends of 70% SRVR/30% FCC HCO. Figure 1 depicts parity graphs of agreement between the measured and predicted viscosities of blends of 70% SRVR/30% FCC HCO by the four SRVR viscosity models. The data in Figure 1 indicated a very good agreement between the measured and predicted viscosities for Models 1, 3, and 4 with the test data, while Model 2 was not as successful in the prediction of viscosity of the blends of 70% SRVR/30% FCC HCO as it was with the training set. For the whole set (training plus test) of 40 data points, the accuracy of prediction decreased in the order: Model 1 (AARE = 14.1%) > Model 4 (16.8%) > Model 2

(18.6%) > Model 3 (25.6%). One may conclude that the molecular weight, specific gravity, and aromatic ring index were the most suitable descriptors of the *SRVR* viscosity, which, along with Model 1 and Model 4, could best predict the viscosities of the *SRVRs*. It is interesting to note here that from the *SRVR* data, specific gravity and molecular weight could be used to predict the viscosity of the 70% *SRVR*/30% *FCC HCO*. Then, the predicted value of viscosity could be used to estimate the C_7 -asphaltene content by Model 2. In other words, the specific gravity and the prediction by Riazi's model of the $T_{50\%}$ of the *SRVR* based on atmospheric residue ASTM D-5236 distillation data were sufficient to predict the *SRVR* C_7 -asphaltene content using Models 1 and 2. Figure 2a presents a graph of agreement between the measured and predicted C_7 -asphaltene content of 40 *SRVRs* through the use of *MW*, *SG*, and Models 1 and 2. For comparison purposes, Figure 2b shows a graph of agreement between the measured and predicted C_7 -asphaltene content of 40 *SRVRs* using the *SRVR* data for density, viscosity of blends of 70% *SRVR*/30% *FCC HCO*, and Conradson carbon content, and the correlation of Samie and Mortaheb [37].

It was observed from these data that Models 1 and 2 and the data for the *MW* and *SG* of the *SRVRs* outperformed the correlation of Samie and Mortaheb [37], with an average absolute relative error = 20.9% for the new method relative to AARE = 32.6% for the correlation of Samie and Mortaheb [37].

Figure 3 presents parity graphs of agreement between the measured and predicted softening points (*SP*) using the three *SRVR SP* models—Models 5, 6, and 7. These data indicated a good agreement between the measured data and that predicted with the test data for softening points, confirming the superiority of Model 6 as established with training set data (Table 13). Therefore, while the viscosity could be best predicted from the *SRVR* data of *MW* and *SG*, the softening point was best predicted from the *SRVR* data of *MW* and C_7 -asphaltene content, with AARE = 10.9% for Model 6, AARE = 12.7% for Model 7, and AARE = 15.0% for Model 5 for all studied 30 *SRVRs*. A total of 23 data sets from Table 2 were used as a training set to develop Models 5, 6, and 7, and 7 data sets were employed as test data.

Figures 4 and 5 show parity graphs of agreement between the measured and predicted viscosity of blends of 70% H-Oil *VTB*/30% *FCC HCO* and the softening points (*SPs*) of H-Oil *VTBs* using Equations (21) and (22). It was evident from these data that there was a very good agreement between the measured and predicted values for both the viscosities and softening points of the H-Oil *VTBs*.

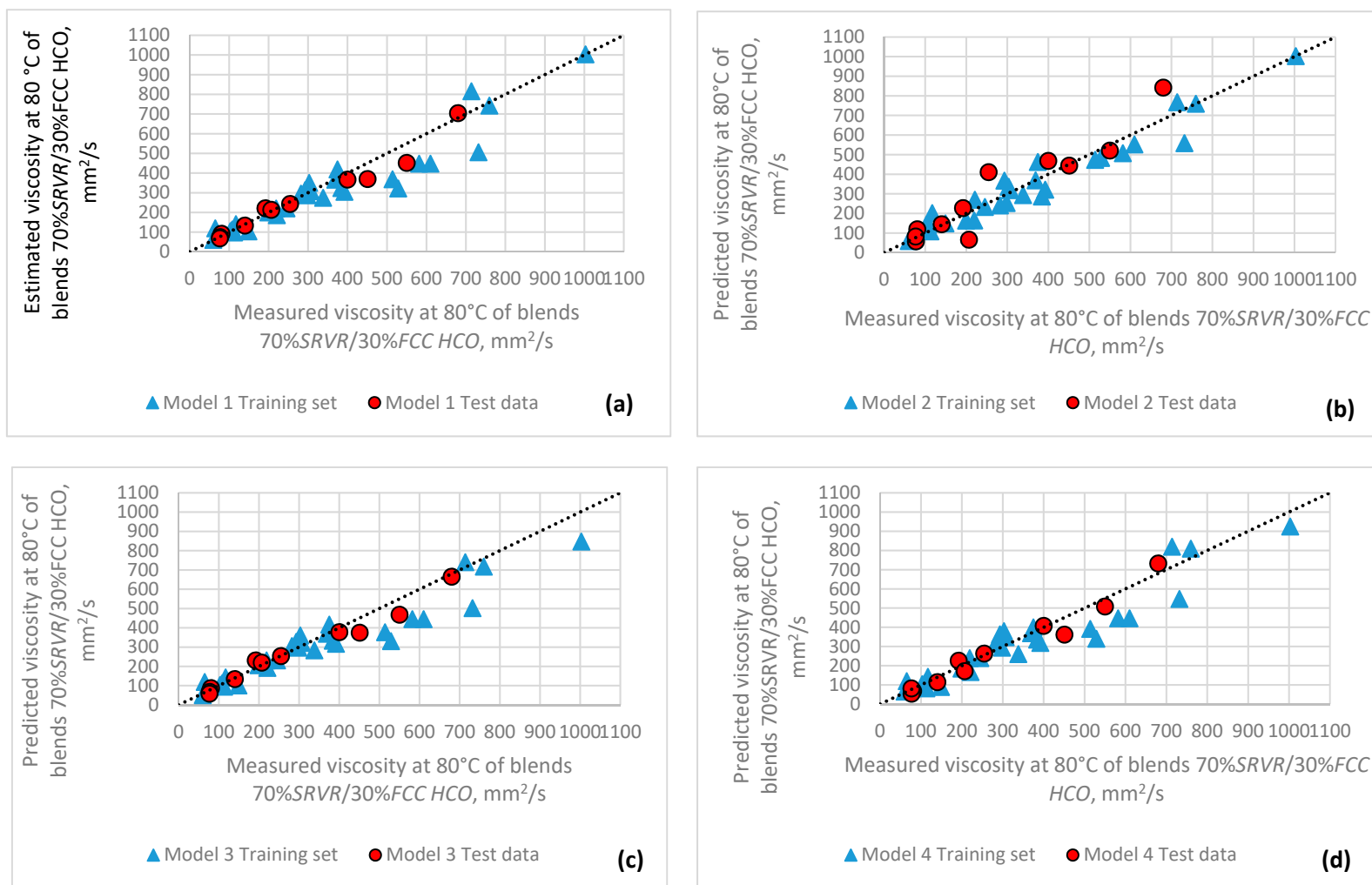
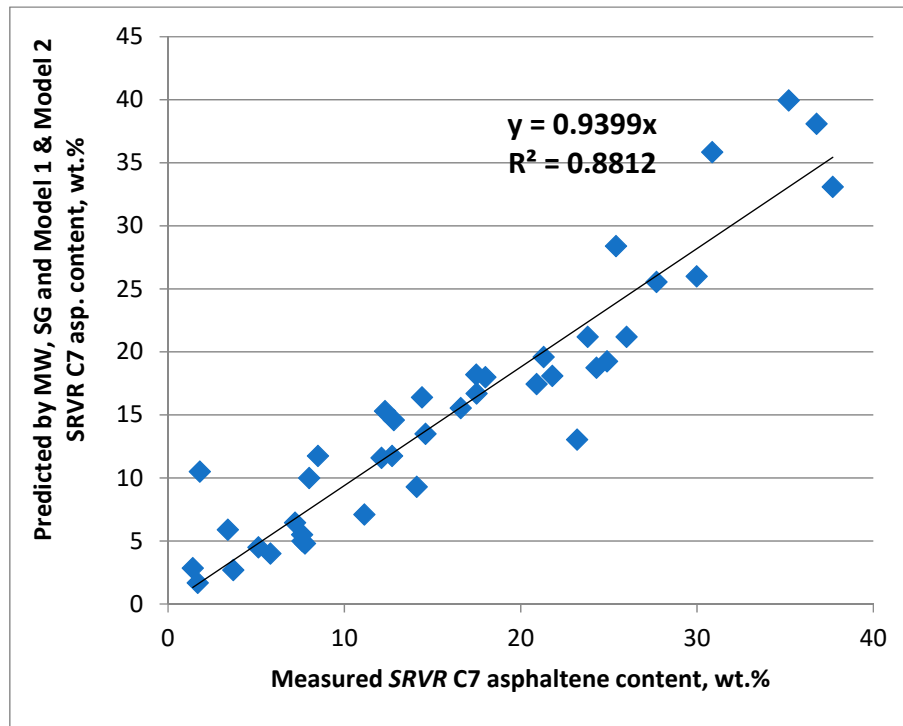
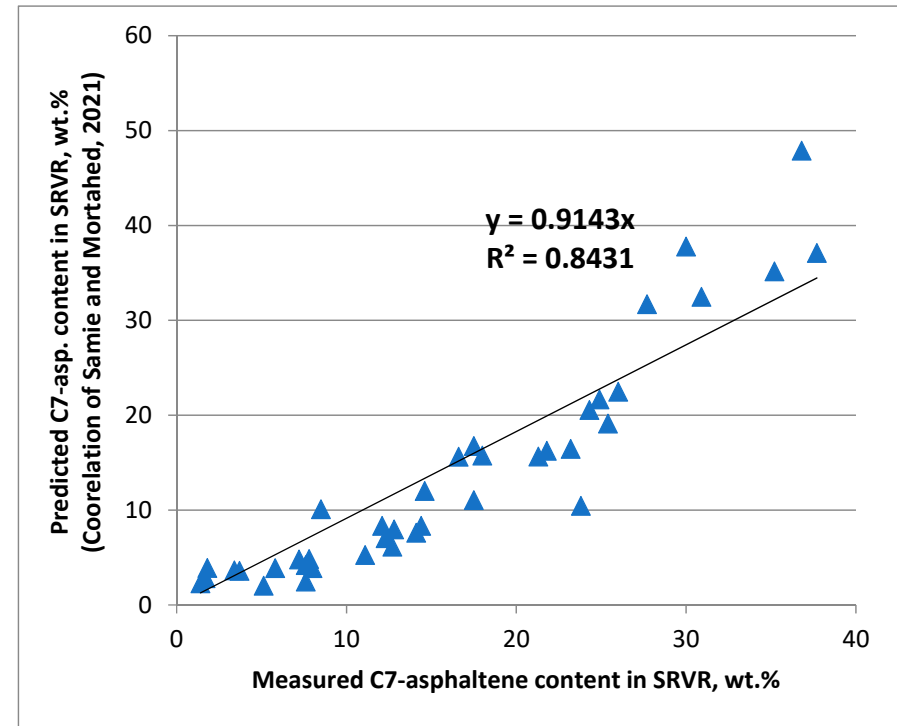


Figure 1. Agreement between measured data and that predicted by Models 1–4 for viscosities of blends of 70% SRVR/30% FCC HCO: (a) Model 1; (b) Model 2; (c) Model 3; (d) Model 4.



(a)



(b)

Figure 2. Agreement between measured data and that predicted by MW, SG, and Model 1 and Model 2 for C₇-asphaltene content in SRVRs (a) and by the correlation of Samie and Mortaheb [37] (b).

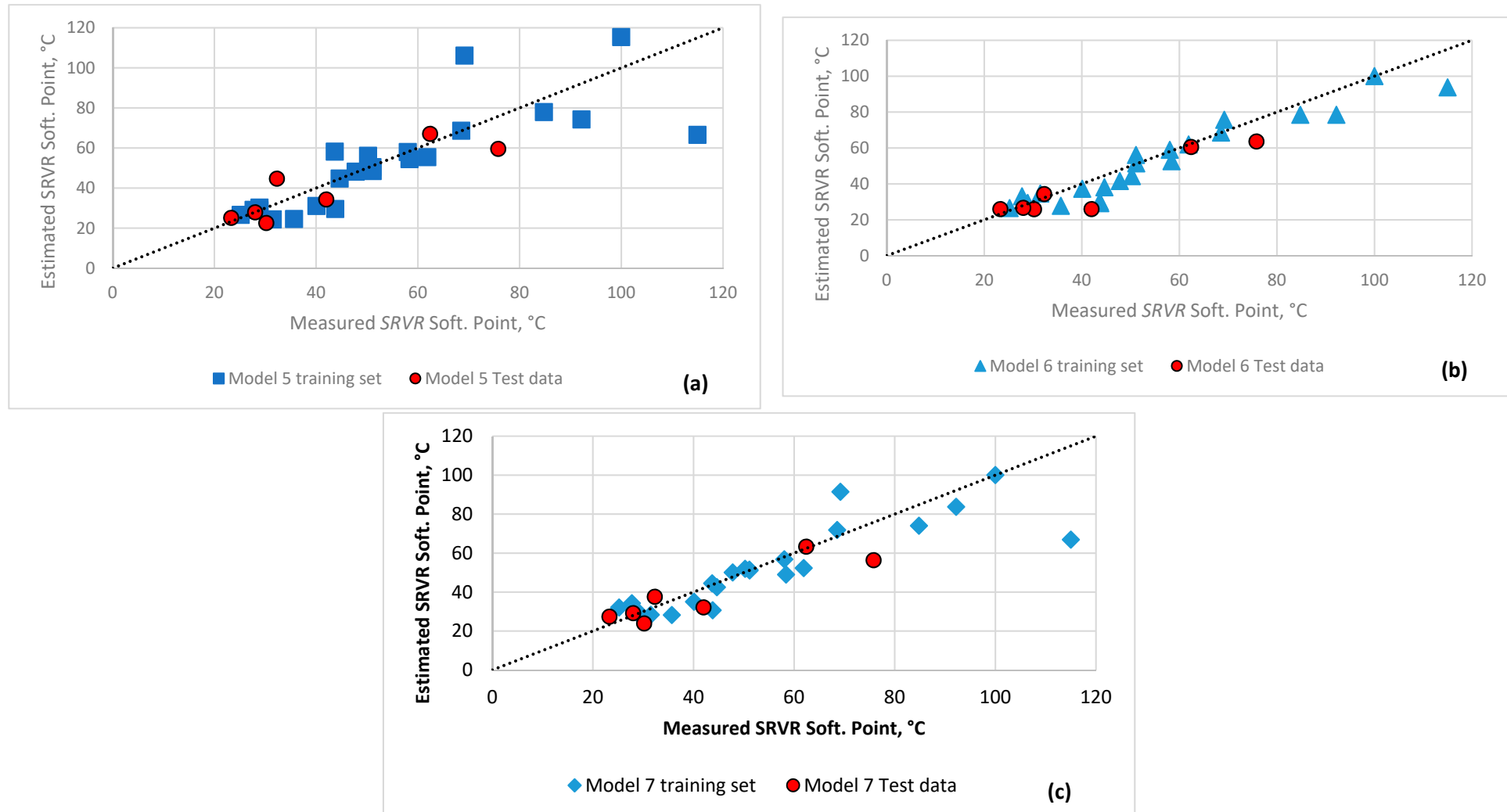


Figure 3. Agreement between measured data and that predicted by Models 5–7 for the softening point of SRVRs: (a) Model 5; (b) Model 6; (c) Model 7.

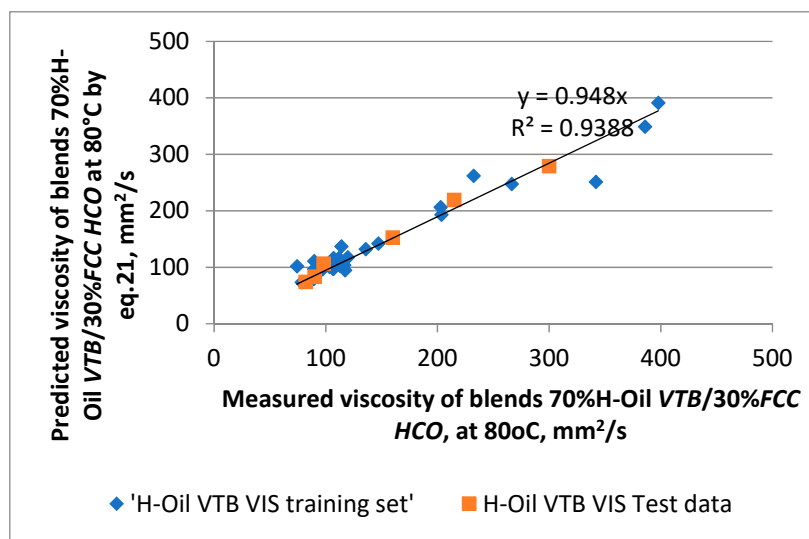


Figure 4. Agreement between measured and predicted viscosities of blends of 70% H-Oil VTB/30%FCC HCO for 33 training set points and 6 test set points using Equation (21).

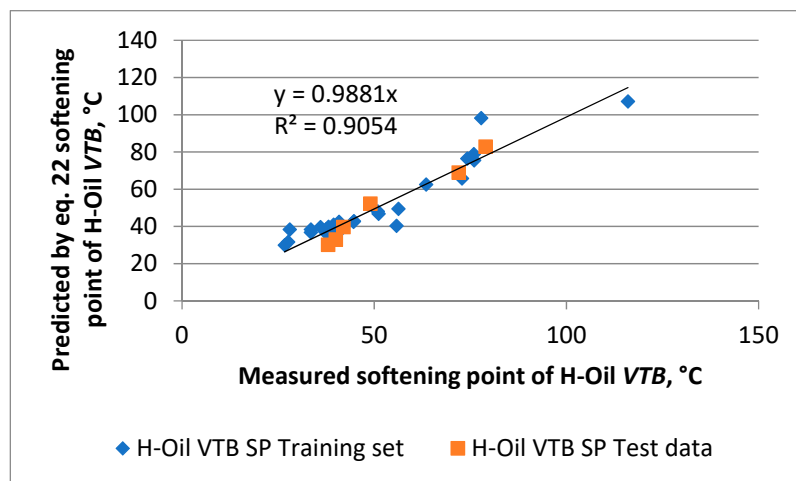


Figure 5. Agreement between measured and predicted softening points of the H-Oil VTB for 33 training set points and 6 test set points using Equation (22).

4. Conclusions

On the basis of the performed investigation, the following conclusions were reached:

1. The molecular weight predicted by the correlation of Linan et al. [27] using specific gravity and the T50% boiling point derived from Riazi's boiling point distribution model for the studied vacuum residues was found to be within the range of molecular weights of distinct vacuum residual oils reported in the literature.
2. The *ICrA* evaluation revealed that the straight-run and hydrocracked (secondary) vacuum residues were completely different, and therefore their viscosities and softening points should be separately modeled.
3. Both the viscosities and softening points of the primary vacuum residues could be modeled using the properties of T50%, molecular weight, C7-asphaltene content, Conradson carbon content, and specific gravity using a Walther's-type equation. The best viscosity model employed the molecular weight and specific gravity, whereas the best *SRVR* softening-point model used the molecular weight and asphaltene content.
4. In addition to the model of Samie and Mortaheb [37], which predicted C7-asphaltene content with an average absolute relative error of 32.6% and used the density, Conradson carbon content, and viscosity of the primary vacuum residue, the C7-asphaltene

content could be also predicted from data for density (specific gravity), T50%, and the viscosities in Models 1 and 2 developed in this work, with an average absolute relative error of 20.9%;

5. The viscosities and softening points of the hydrocracked vacuum residues could be modeled from a single property—the Conradson carbon content.
6. The vacuum residue viscosity modeled in this research was related to the viscosity of blends of primary and secondary vacuum residue (70%) and FCC HCO (30%) due to the uncertainty of the measurements of viscosities of highly viscous vacuum residua. An investigation of the suitability of blending models available in the literature to the studied blends of vacuum residua (70%) and FCC HCO (30%) to determine the viscosities of the pure primary and secondary vacuum residua will be a subject of a future work.

Supplementary Materials: The following supporting information can be downloaded at: <https://www.mdpi.com/article/10.3390/en15051755/s1>, Table S1: ASTM D 5236 physical vacuum distillation data of the atmospheric residues from the studied 30 crude oils; Table S2: High-temperature simulated distillation (HTSD, ASTM D 7169) of some of the studied SRVRs; Table S3: HTSD characteristics of the 33 studied H-Oil ATBs; Table S4: A comparison between the distillation characteristics of the two H-Oil VTBs extrapolated by Riazi’s distribution model applied to the data of the physical vacuum distillation (ASTM D 5236) and of the gas chromatographic HTSD (ASTM D 7169).

Author Contributions: Conceptualization, E.S.; Data curation, S.N. and R.D.; Formal analysis, D.Y.; Investigation, D.D.S. (Denis D. Stratiev) and L.T.-Y.; Methodology, S.S. and N.A.A.; Software, V.A., D.N., S.R. and D.D.S. (Danail D. Stratiev); Supervision, K.A.; Writing—original draft, D.S., S.N. and I.S. All authors have read and agreed to the published version of the manuscript.

Funding: This research was funded by project UNITE BG05M2OP001-1.001-0004/28.02.2018 (2018–2023).

Institutional Review Board Statement: Not applicable.

Informed Consent Statement: Not applicable.

Data Availability Statement: Not applicable.

Acknowledgments: K.A. acknowledges the support from the project UNITE BG05M2OP001-1.001-0004/28.02.2018 (2018–2023).

Conflicts of Interest: The authors declare no conflict of interest.

Nomenclature

<i>AARE</i>	Average absolute relative error, %
<i>ABP</i>	Average boiling point
<i>API</i>	API gravity
<i>ARI</i>	Aromatic ring index
<i>ATB</i>	Atmospheric tower bottom product
<i>CCR</i>	Conradson carbon content, wt. %
d_{15}	Density at 15 °C, g/cm ³
<i>E</i>	Error
<i>FBP</i>	Final boiling point, °C
<i>FCC</i>	Fluid catalytic cracking
<i>HCO</i>	Heavy cycle oil
<i>HNR</i>	Highest number residual
<i>ICrA</i>	Intercriteria analysis
<i>IBP</i>	Initial boiling point, °C
<i>LNB</i>	LUKOIL Neftohim Burgas
<i>LNR</i>	Lowest number residual
<i>MAX E</i>	Maximum error
<i>MIN E</i>	Minimum error
<i>MW</i>	Molecular weight,

nD_{20}	Refractive index at 20 °C
R	Residual
#R+	Number of positive residuals
#R−	Number of negative residuals
RSE	Relative standard error
SE	Standard error
SG	Specific gravity
SP	Softening point
SRVR	Straight-run vacuum residue
SSE	Sum of squared errors
VIS	Kinematic viscosity, cSt
VR	Vacuum residue
VTB	Vacuum tower bottom product

References

- Stanislaus, A.; Hauser, A.; Marafi, M. Investigation of the mechanism of sediment formation in residual oil hydrocracking process through characterization of sediment deposits. *Catal. Today* **2005**, *109*, 167–177. [\[CrossRef\]](#)
- Pang, W.-W.; Kuramae, M.; Kinoshita, Y.; Lee, J.-K.; Zhang, Y.Z.; Yoon, S.-H.; Mochida, I. Plugging problems observed in severe hydrocracking of vacuum residue. *Fuel* **2009**, *88*, 663–669. [\[CrossRef\]](#)
- Stratiev, D.; Dinkov, R.; Shishkova, I.; Sharafutdinov, I.; Ivanova, N.; Mitkova, M.; Yordanov, D.; Rudnev, N.; Stanulov, K.; Artemiev, A.; et al. What is behind the high values of hot filtration test of the ebullated bed residue H-Oil hydrocracker residual oils? *Energy Fuels* **2016**, *30*, 7037–7054. [\[CrossRef\]](#)
- Miller, K.A.; Nelson, L.A.; Almond, R.M. Should You Trust Your Heavy Oil Viscosity Measurement? *J. Can. Pet. Technol.* **2006**, *45*, 42–48. [\[CrossRef\]](#)
- Stratiev, D.; Shishkova, I.; Nikolaychuk, E.; Atanasova, V.; Atanassov, K. Investigation of relations of properties of straight run and H-Oil unconverted vacuum residual oils. *Pet. Coal* **2019**, *61*, 763–776.
- Carbognani, L.; Carbognani-Arambarri, L.; Lopez-Linares, F.; Pereira-Almao, P. Suitable Density Determination for Heavy Hydrocarbons by Solution Pycnometry: Virgin and Thermal Cracked Athabasca Vacuum Residue Fractions. *Energy Fuels* **2011**, *25*, 3663–3670. [\[CrossRef\]](#)
- Mullins, O.C.; Sheu, E.Y.; Hammami, A.; Marshall, A.G. *Asphaltenes, Heavy Oils and Petroleomics*; Springer: New York, NY, USA, 2007.
- Ruiz-Morales, Y.; Mullins, O.C. Polycyclic aromatic hydrocarbons of asphaltenes analyzed by molecular orbital calculations with optical spectroscopy. *Energy Fuels* **2007**, *21*, 256–265. [\[CrossRef\]](#)
- Chacón-Patiño, M.L.; Rowland, S.M.; Rodgers, R.P. Advances in asphaltene petroleomics. Part 1: Asphaltenes are composed of abundant island and archipelago structural motifs. *Energy Fuels* **2017**, *31*, 13509–13518. [\[CrossRef\]](#)
- Chacón-Patiño, M.L.; Rowland, S.M.; Rodgers, R.P. Advances in Asphaltene Petroleomics. Part 2: Selective Separation Method That Reveals Fractions Enriched in Island and Archipelago Structural Motifs by Mass Spectrometry. *Energy Fuels* **2018**, *32*, 314–328. [\[CrossRef\]](#)
- Chacón-Patiño, M.L.; Rowland, S.M.; Rodgers, R.P. Advances in Asphaltene Petroleomics. Part 3. Dominance of Island or Archipelago Structural Motif Is Sample Dependent. *Energy Fuels* **2018**, *32*, 9106–9120. [\[CrossRef\]](#)
- Mullins, O.C. The modified Yen model. *Energy Fuels* **2010**, *24*, 2179–2207. [\[CrossRef\]](#)
- Mullins, O.C.; Sabbah, H.; Eyssautier, J.; Pomerantz, A.E.; Barré, L.; Andrews, A.B.; Ruiz-Morales, Y.; Mostowfi, F.; McFarlane, R.; Goual, L.; et al. Advances in asphaltene science and the Yen—Mullins model. *Energy Fuels* **2012**, *26*, 3986–4003. [\[CrossRef\]](#)
- Mullins, O.C.; Martinez-Haya, B.; Marshall, A.G. Contrasting perspective on asphaltene molecular weight. this comment vs. the overview of Herod, A.A., Bartle, K.D., Kandiyoti, R. *Energy Fuels* **2008**, *22*, 1765–1773. [\[CrossRef\]](#)
- Badre, S.; Goncalves, C.C.; Norinaga, K.; Gustavson, G.; Mullins, O.C. Comment on Molecular size and weight of asphaltene and asphaltene solubility fractions from coals, crude oils and bitumen. *Fuel* **2006**, *85*, 1950–1951. [\[CrossRef\]](#)
- Buch, L.; Groenzin, H.; Buenrostro-Gonzales, E.; Andersen, S.I.; Lira-Galeana, C.; Mullins, O.C. Molecular size of asphaltene fractions obtained from residuum hydrotreatment. *Energy Fuels* **2003**, *82*, 1075–1084. [\[CrossRef\]](#)
- Wiehe, I.A. A Solvent-Resid Phase Diagram for Tracking Resid Conversion. *Ind. Eng. Chem. Res.* **1992**, *31*, 530–536. [\[CrossRef\]](#)
- Strausz, O.P.; Safarik, I.; Lown, E.M.; Morales-Izquierdo, A. A critique of asphaltene fluorescence decay and depolarization-based claims about molecular weight and molecular architecture. *Energy Fuels* **2008**, *22*, 1156–1166. [\[CrossRef\]](#)
- Akbarzadeh, K.; Alboudwarej, H.; Svrcek, W.Y.; Yarranton, H.W. A generalized regular solution model for asphaltene precipitation from n-alkane diluted heavy oils and bitumens. *Fluid Phase Equilib.* **2005**, *232*, 159–170. [\[CrossRef\]](#)
- Schucker, R.C. Thermogravimetric determination of the coking kinetics of Arab Heavy vacuum residuum. *Ind. Eng. Chem. Process Des. Dev.* **1983**, *22*, 615–619. [\[CrossRef\]](#)
- Liang, W.; Que, G.; Chen, Y.; Liu, C. *Chemical Composition and Characteristics of Residues of Chinese Crude Oils, Asphaltenes and Asphalts. 2. Developments in Petroleum Science*; Elsevier Science B.V.: Amsterdam, The Netherlands, 2000.
- León, A.Y.; Parra, M.; Grosso, J.L. Estimation of critical properties of typically Colombian vacuum residue SARA fractions. *CTF-Cienc. Tecnol. Futuro* **2008**, *3*, 129–142.

23. Sheremata, J.M.; Gray, M.R.; Dettman, H.D.; McCaffrey, W.C. Quantitative Molecular Representation and Sequential Optimization of Athabasca Asphaltenes. *Energy Fuels* **2004**, *18*, 1377–1384. [[CrossRef](#)]
24. Goossens, A.G. Prediction of Molecular Weight of Petroleum Fractions. *Ind. Eng. Chem. Res.* **1996**, *35*, 985–988. [[CrossRef](#)]
25. Riazi, M.R.; Daubert, T.E. Characterization Parameters for Petroleum Fractions. *Ind. Eng. Chem. Res.* **1987**, *26*, 755–759. [[CrossRef](#)]
26. Riazi, M.R. *Characterization and Properties of Petroleum Fraction*; ASTM manual series MNL50; ASTM International: Philadelphia, PA, USA, 2005.
27. Liñan, L.Z.; Lima, N.M.N.; Maciel, M.R.W.; Filho, R.M.; Medina, L.C.; Embiruçu, M. Correlation for predicting the molecular weight of Brazilian petroleum residues and cuts: An application for the simulation of a molecular distillation process. *J. Pet. Sci. Eng.* **2011**, *78*, 78–85. [[CrossRef](#)]
28. Stratiev, D.S.; Shishkova, I.K.; Dinkov, R.K.; Petrov, I.P.; Kolev, I.V.; Yordanov, D.; Sotirov, S.; Sotirova, E.; Ribagin, S.; Atanassov, K.; et al. Empirical Models to Characterize the Structural and Physicochemical Properties of Vacuum Gas Oils with Different Saturate Contents. *Resources* **2021**, *10*, 71. [[CrossRef](#)]
29. Stratiev, D.S.; Nenov, S.; Shishkova, I.K.; Dinkov, R.K.; Zlatanov, K.; Yordanov, D.; Sotirov, S.; Sotirova, E.; Atanassova, V.; Atanassov, K.; et al. Comparison of Empirical Models to Predict Viscosity of Secondary Vacuum Gas Oils. *Resources* **2021**, *10*, 82. [[CrossRef](#)]
30. Liu, Q.; Yang, S.; Liu, Z.; Liu, Q.; Shi, L.; Wei Han, W.; Zhang, L.; Li, M. Comparison of TG-MS and GC-simulated distillation for determination of the boiling point distribution of various oils. *Fuel* **2021**, *301*, 121088. [[CrossRef](#)]
31. Carbognani Ortega, L.A.; Carbognani, J.; Pereira Almas, P.P. The Boduszynski Continuum: Contributions to the Understanding of the Molecular Composition of Petroleum Chapter 10. In *Correlation of Thermogravimetry and High Temperature Simulated Distillation for Oil Analysis: Thermal Cracking Influence over both Methodologies*; American Chemical Society: Washington, DC, USA, 2018; pp. 223–239. [[CrossRef](#)]
32. Stratiev, D.S.; Dinkov, R.K.; Shishkova, I.K.; Nedelchev, A.D.; Tasaneva, T.; Nikolaychuk, E.; Sharafutdinov, I.M.; Rudney, N.; Nenov, S.; Mitkova, M.; et al. An Investigation on the Feasibility of Simulating the Distribution of the Boiling Point and Molecular Weight of Heavy Oils. *Pet. Sci. Technol.* **2015**, *33*, 527–541. [[CrossRef](#)]
33. Wiehe, I.A. Asphaltene Solubility and Fluid Compatibility. *Energy Fuels* **2012**, *26*, 4004–4016. [[CrossRef](#)]
34. Sánchez-Lemus, M.C.; Okafor, J.C.; Ortiz, D.P.; Schoegg, F.F.; Taylor, S.D.; van den Berg, F.G.A. Improved density prediction for mixtures of native and refined heavy oil with solvents. *Energy Fuels* **2015**, *29*, 3052–3063. [[CrossRef](#)]
35. Sánchez-Lemus, M.C.; Schoegg, F.; Taylor, S.D.; Yarranton, H.W. Physical properties of heavy oil distillation cuts. *Fuel* **2016**, *180*, 457–472. [[CrossRef](#)]
36. Zhao, H.; Memon, A.; Gao, J.; Taylor, S.D.; Sieben, D.; Ratulowski, J.; Alboudwarej, H.; Pappas, J.; Creek, J.L. Heavy Oil Viscosity Measurements—Best Practices and Guidelines. *Energy Fuels* **2016**, *30*, 5277–5290. [[CrossRef](#)]
37. Samie, M.S.; Mortaheb, H.R. Novel correlations for prediction of SARA contents of vacuum residues. *Fuel* **2021**, *305*, 121609. [[CrossRef](#)]
38. Stratiev, D.; Shishkova, I.; Dinkov, R.; Kirilov, K.; Yordanov, D.; Nikolova, R.; Veli, A.; Tavlieva, M.; Vasilev, S.; Suyunov, R. Variation of oxidation reactivity of straight run and H-Oil hydrocracked vacuum residual oils in the process of road asphalt production. *Road Mater. Pavement Des.* **2021**, 1–25. [[CrossRef](#)]
39. Stratiev, D.; Dinkov, R.; Shishkova, I.; Kirilov, K.; Yordanov, D.; Ilchev, I.; Toteva, V. Laboratory and commercial investigation on the production of road asphalt from blends of straight run and hydrocracked vacuum residua in different ratios. *Oxid. Commun.* **2021**, *44*, 652–663.
40. Stratiev, D.; Shishkova, I.; Nikolaychuk, E.; Ijlstra, W.; Holmes, B.; Caillot, M. Feed properties effect on the performance of vacuum residue ebullated bed H-Oil hydrocracking. *Oil Gas Eur. Mag.* **2019**, *45*, 194–200.
41. Stratiev, D.; Shishkova, I.; Nikolova, R.; Tsaneva, T.; Mitkova, M.; Yordanov, D. Investigation on precision of determination of SARA analysis of vacuum residual oils from different origin. *Pet. Coal* **2016**, *58*, 109–119.
42. Stratiev, D.; Shishkova, I.; Tsaneva, T.; Mitkova, M.; Yordanov, D. Investigation of relations between properties of vacuum residual oils from different origin, and of their deasphalted and asphaltene fractions. *Fuel* **2016**, *170*, 115–129. [[CrossRef](#)]
43. Diarov, I.N.; Batueva, I.U.; Sadikov, A.N.; Colodova, N.L. *Chemistry of Crude Oil*; Chimia Publishers: St. Peterburg, Russia, 1990. (In Russian)
44. BDS (Bulgarian Standard) EN 1427:2015. *Bitumen and Bituminous Binders—Determination of the Softening Point—Ring and Ball Method*; BDS: Sofia, Bulgaria, 2015.
45. Abutaqiya, M. Advances in Thermodynamic Modeling of Nonpolar Hydrocarbons and Asphaltene Precipitation in Crude Oils. Ph.D. Thesis, Rice University, Houston, TX, USA, 2019.
46. Abutaqiya, M.I.L.; AlHammadi, A.A.; Sisco, C.J.; Vargas, F.M. Aromatic ring index (ARI): A Characterization factor for nonpolar hydrocarbons from molecular weight and refractive index. *Energy Fuels* **2021**, *35*, 1113–1119. [[CrossRef](#)]
47. Stratiev, D.S.; Marinov, I.M.; Shishkova, I.K.; Dinkov, R.K.; Stratiev, D.D. Investigation on feasibility to predict the content of saturate plus mono-nuclear aromatic hydrocarbons in vacuum gas oils from bulk properties and empirical correlations. *Fuel* **2014**, *129*, 156–162. [[CrossRef](#)]
48. Hernández, E.A.; Sánchez-Reyna, G.; Ancheyta, J. Comparison of mixing rules based on binary interaction parameters for calculating viscosity of crude oil blends. *Fuel* **2019**, *249*, 198–205. [[CrossRef](#)]
49. Burnham, K.P.; Anderson, D.R. *Model Selection and Multimodel Inference*, 2nd ed.; Springer: New York, NY, USA, 2002.

50. van den Berg, F.G.A.; Heijnis, R.M.A.; Stamps, P.A.; Kramer, P.A. A Geochemical Framework for Understanding Residue Properties. *Pet. Sci. Technol.* **2003**, *21*, 449–460. [[CrossRef](#)]
51. Dreillard, M.; Marques, J.; Barbier, J.; Feugnet, F. The Chateaux at Deer Valley. In Proceedings of the Petrophase Conference, Park City, UT, USA, 8–12 July 2018.
52. Redelius, P.; Soenen, H. Relation between bitumen chemistry and performance. *Fuel* **2015**, *140*, 34–43. [[CrossRef](#)]
53. Walther, C. Ueber die Auswertung von Viskositätsangaben. *Erdoel Teer* **1931**, *7*, 382–384.
54. Stratiev, D.; Nenov, S.; Nedanovski, D.; Shishkova, I.; Dinkov, R.; Stratiev, D.D.; De Stratiev, D.; Atanassov, K.; Yordanov, D.; Angelova, N.A. Different nonlinear regression techniques and sensitivity analysis as tools to optimize oil viscosity modeling. *Resources* **2021**, *10*, 99. [[CrossRef](#)]
55. Stratiev, D.; Nedelchev, A.; Shishkova, I.; Ivanov, A.; Sharafutdinov, I.; Nikolova, R.; Mitkova, M.; Yordanov, D.; Rudnev, N.; Belchev, Z.; et al. Dependence of visbroken residue viscosity and vacuum residue conversion in a commercial visbreaker unit on feedstock quality. *Fuel Process. Technol.* **2015**, *138*, 595–604. [[CrossRef](#)]